

Probing the Neutron Skin Puzzle in ^{208}Pb : precision polarized electron scattering at Mainz

N. Kozyrev, A. Esser, M. Hoek, M. Thiel, and C. Sfienti

Institut für Kernphysik, Johannes Gutenberg-Universität, Mainz, Germany

CRC 1660 Annual Graduate School
22 – 26 September 2025

JOHANNES GUTENBERG
UNIVERSITÄT MAINZ



Cluster of Excellence

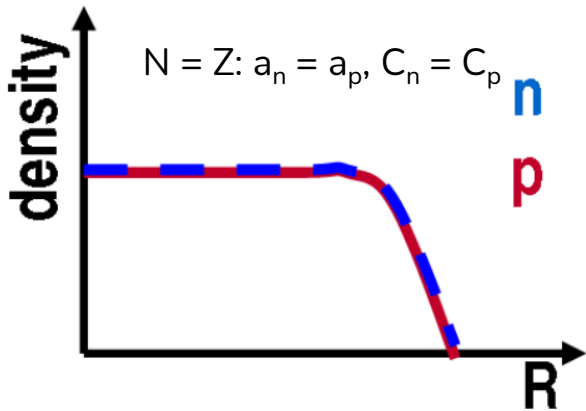
PRISMA+

Precision Physics,
Fundamental Interactions
and Structure of Matter

Outline

- Neutron skin and Nuclear Equation of State (EoS)
- Parity-violating electron scattering (PVeS) and the MREX experiment
- Beam-normal single spin asymmetry and the latest A1 experiment results

Connecting different scales through EoS

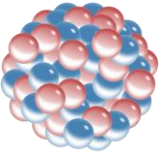


J. Phys. G, **46** (2019), 093003

$$\rho(r) = \frac{\rho_0}{1 + \exp[(r - C)/a]} \quad \text{— 2pF density distribution}$$

$$\Delta r_{np} = R_{skin} = R_n - R_p \quad \text{— NS thickness}$$

$$R_n = \sqrt{\langle r_n^2 \rangle}, \quad R_p = \sqrt{\langle r_p^2 \rangle}$$



Neutron skin in nuclei

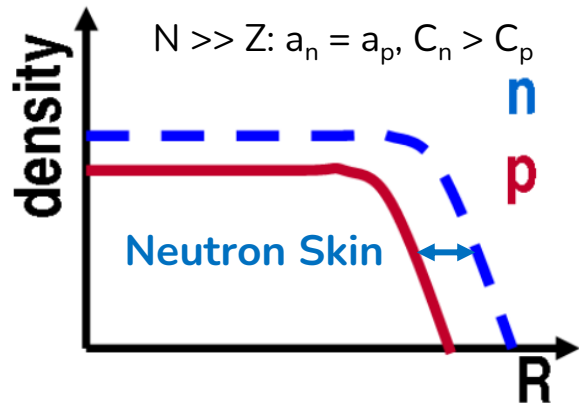
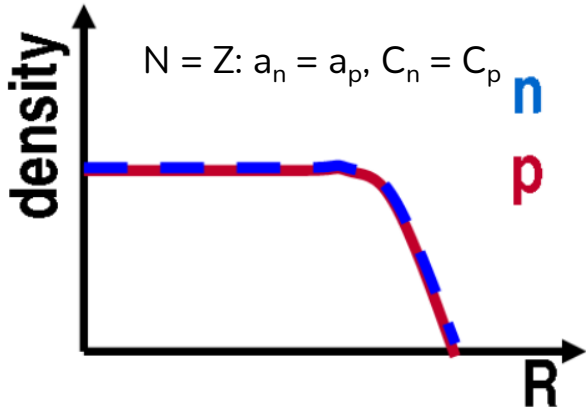


Fig. Schematic representation of neutron and proton density distributions in nuclei

Connecting different scales through EoS



J. Phys. G, **46** (2019), 093003

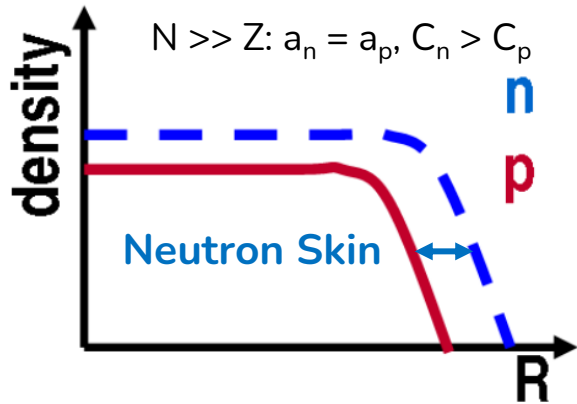
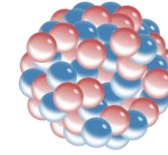


Fig. Schematic representation of neutron and proton density distributions in nuclei

$$\rho(r) = \frac{\rho_0}{1 + \exp[(r - C)/a]} \quad \text{— 2pF density distribution}$$

$$\Delta r_{np} = R_{skin} = R_n - R_p \quad \text{— NS thickness}$$

$$R_n = \sqrt{\langle r_n^2 \rangle}, \quad R_p = \sqrt{\langle r_p^2 \rangle}$$



Neutron skin in nuclei



Nuclear EoS

$$\mathcal{E}(\rho, \alpha) = \mathcal{E}_{\text{SNM}}(\rho) + \alpha^2 \mathcal{S}(\rho) + \mathcal{O}(\alpha^4), \quad \alpha \equiv (\rho_n - \rho_p) / (\rho_n + \rho_p)$$

$$\mathcal{S}(\rho) = J + Lx + \frac{1}{2} K_{\text{sym}} x^2 + \dots, \quad x = (\rho - \rho_0) / 3\rho_0$$

$$L \equiv 3\rho_0 \left. \left(\frac{\partial \mathcal{S}}{\partial \rho} \right) \right|_{\rho_0} \quad \text{— symmetry energy slope parameter}$$

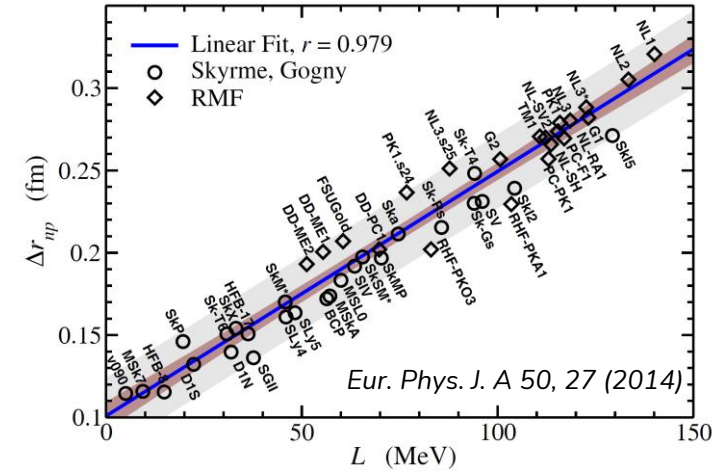
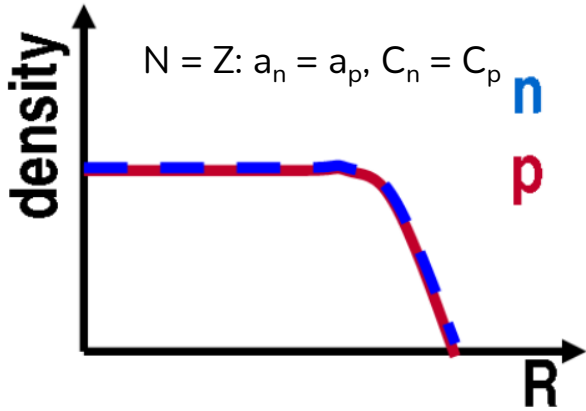


Fig. Correlation between R_{skin} in ^{208}Pb and L produced by different models

Connecting different scales through EoS



J. Phys. G, 46 (2019), 093003

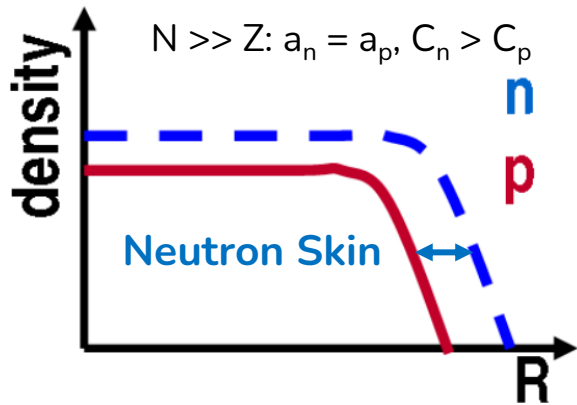


Fig. Schematic representation of neutron and proton density distributions in nuclei



$$\rho(r) = \frac{\rho_0}{1 + \exp[(r - C)/a]} \quad \text{— 2pF density distribution}$$

$$\Delta r_{np} = R_{skin} = R_n - R_p \quad \text{— NS thickness}$$

$$R_n = \sqrt{\langle r_n^2 \rangle}, \quad R_p = \sqrt{\langle r_p^2 \rangle}$$

Neutron skin in nuclei



Nuclear EoS

$$\mathcal{E}(\rho, \alpha) = \mathcal{E}_{SNM}(\rho) + \alpha^2 \mathcal{S}(\rho) + \mathcal{O}(\alpha^4), \quad \alpha \equiv (\rho_n - \rho_p) / (\rho_n + \rho_p)$$

$$\mathcal{S}(\rho) = J + Lx + \frac{1}{2} K_{sym} x^2 + \dots, \quad x = (\rho - \rho_0) / 3\rho_0$$

$$L \equiv 3\rho_0 \left. \left(\frac{\partial \mathcal{S}}{\partial \rho} \right) \right|_{\rho_0} \quad \text{— symmetry energy slope parameter}$$



Neutron star

$$\Lambda(\text{LIGO-Virgo}) \quad \Lambda = \frac{2}{3} k_2 \left(\frac{c^2 R}{GM} \right)^5$$

$$R(\text{NICER})$$

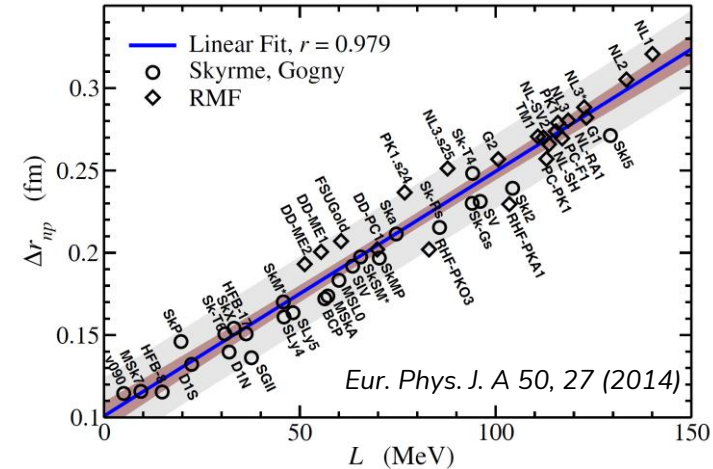


Fig. Correlation between R_{skin} in ^{208}Pb and L produced by different models

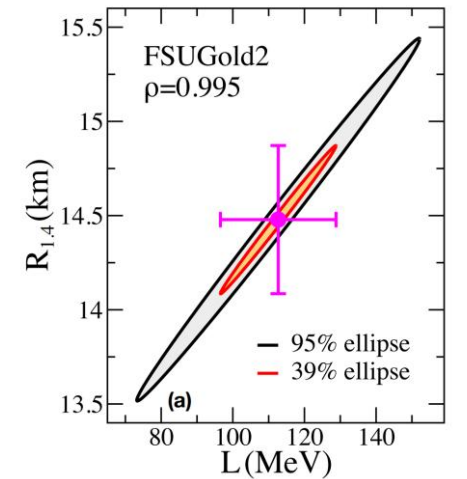


Fig. Dependence between L and $R_{1.4M_\odot}$ in FSUGold2

Parity-violating electron scattering

- Weak force violates parity
- Interference of virtual γ and Z^0 exchange

$$A_{\text{PV}} = \frac{\sigma_R - \sigma_L}{\sigma_R + \sigma_L} \approx \frac{G_F Q^2 |Q_W| F_W(Q^2)}{4\sqrt{2} \pi \alpha Z F_{\text{ch}}(Q^2)}$$



Weak (neutron) radius extraction

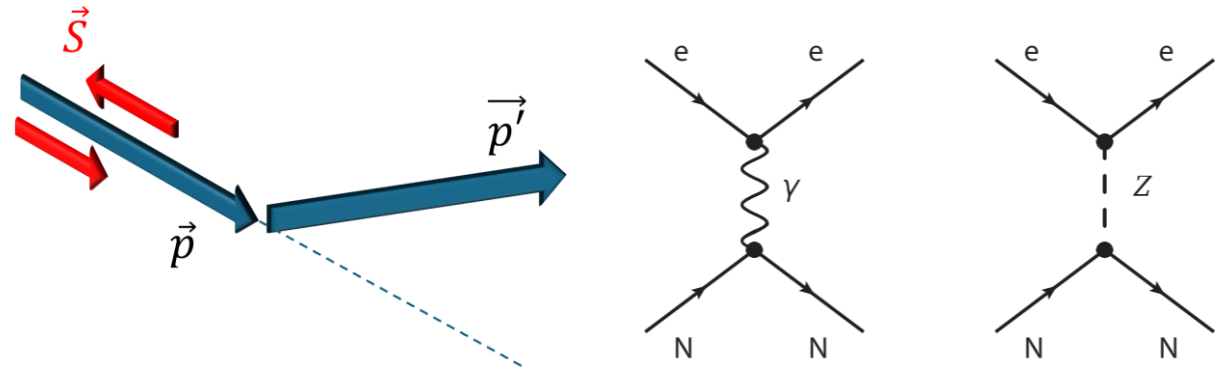


Fig. Polarized electron scattering of nucleus through γ and Z^0 exchange

Parity-violating electron scattering

- Weak force violates parity
- Interference of virtual γ and Z^0 exchange

$$A_{PV} = \frac{\sigma_R - \sigma_L}{\sigma_R + \sigma_L} \approx \frac{G_F Q^2 |Q_W| F_W(Q^2)}{4\sqrt{2} \pi \alpha Z F_{ch}(Q^2)}$$



Weak (neutron) radius extraction

PREX-II (^{208}Pb): $\Delta r_{np} = 0.28 \pm 0.07$ fm

- High statistical uncertainty
- Unexpectedly thick NS (stiff EoS)
- Contradicts CREX in L

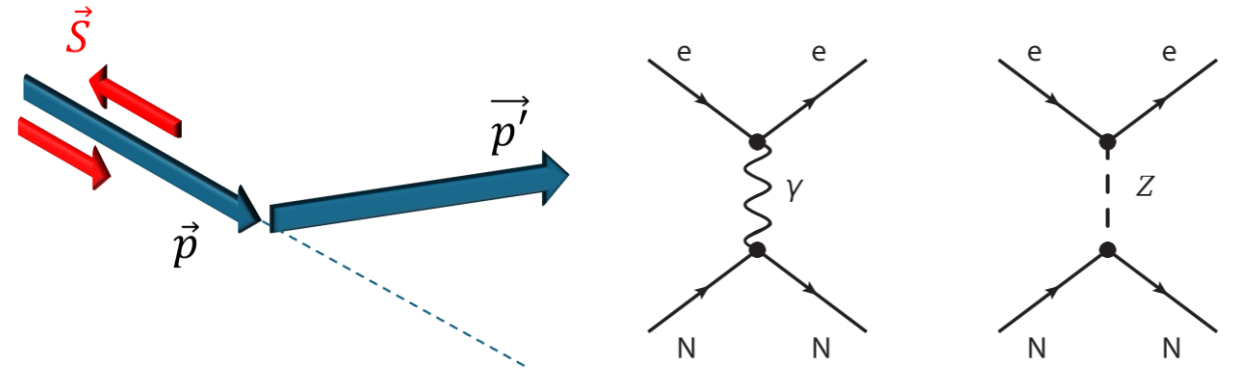


Fig. Polarized electron scattering of nucleus through γ and Z^0 exchange

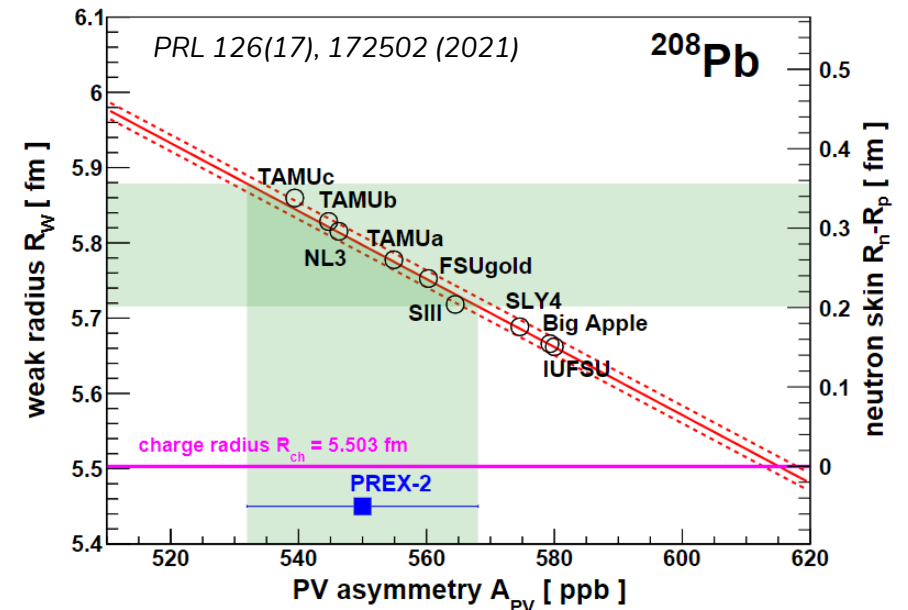


Fig. Correlation between A_{PV} , R_W and Δr_{np} in ^{208}Pb at PREX

Parity-violating electron scattering

- Weak force violates parity
- Interference of virtual γ and Z^0 exchange

$$A_{PV} = \frac{\sigma_R - \sigma_L}{\sigma_R + \sigma_L} \approx \frac{G_F Q^2 |Q_W| F_W(Q^2)}{4\sqrt{2} \pi \alpha Z F_{ch}(Q^2)}$$



Weak (neutron) radius extraction

PREX-II (^{208}Pb): $\Delta r_{np} = 0.28 \pm 0.07$ fm

- High statistical uncertainty
- Unexpectedly thick NS (stiff EoS)
- Contradicts CREX in L



Goal: 0.5% in R_n
(double the
PREX precision)

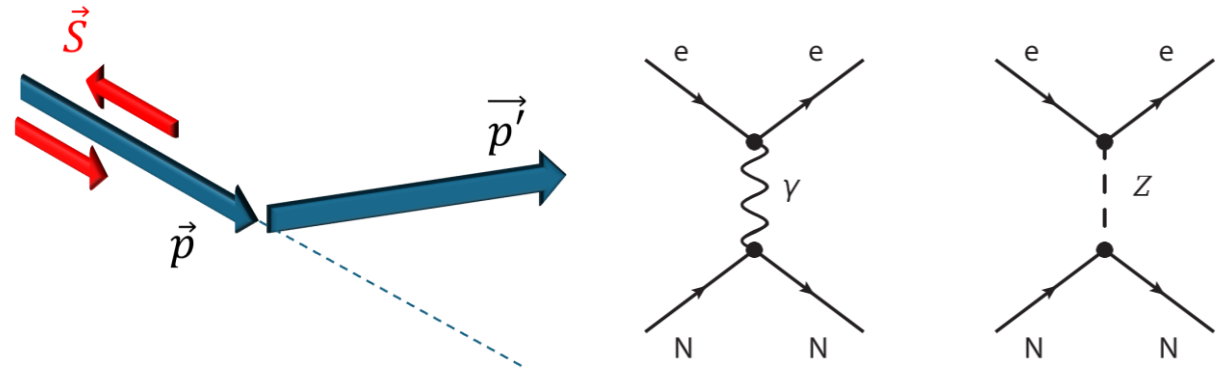


Fig. Polarized electron scattering of nucleus through γ and Z^0 exchange

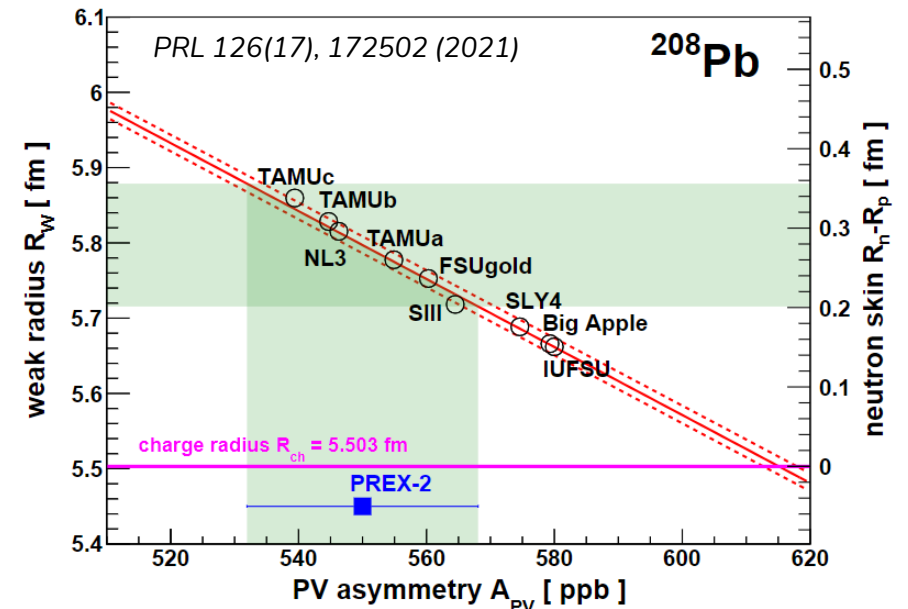


Fig. Correlation between A_{PV} , R_W and Δr_{np} in ^{208}Pb at PREX

Outline for MREX experiment

Mainz Energy-recovering Superconducting Accelerator (MESA):

- 150 μA polarized electron beam with $E_{\text{kin}} = 155 \text{ MeV}$
- Polarization measurement with $<1\%$ uncertainty

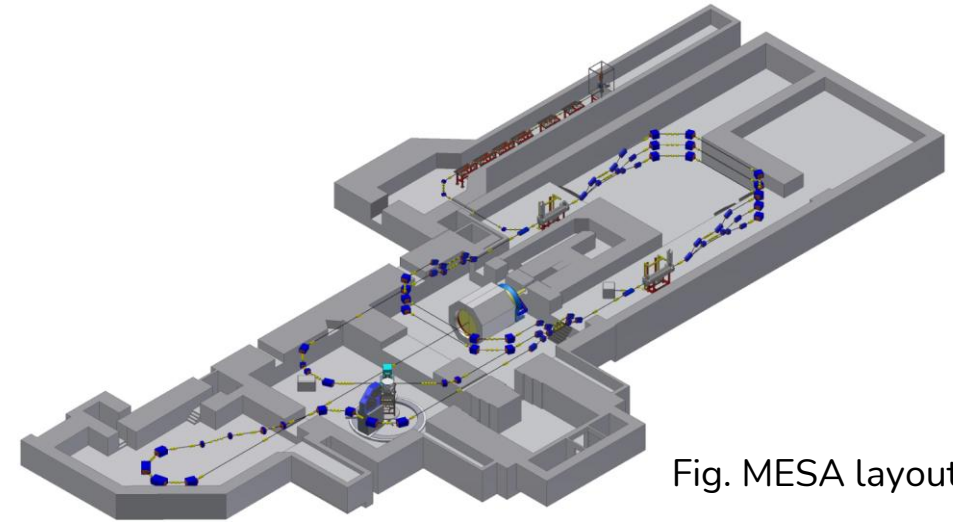


Fig. MESA layout

Outline for MREX experiment

Mainz Energy-recovering Superconducting Accelerator (MESA):

- 150 μA polarized electron beam with $E_{\text{kin}} = 155 \text{ MeV}$
- Polarization measurement with $<1\%$ uncertainty

P2 experiment:

- High-precision measurement of $\sin^2\theta_W$
- Exchange hydrogen with ^{208}Pb for MREX

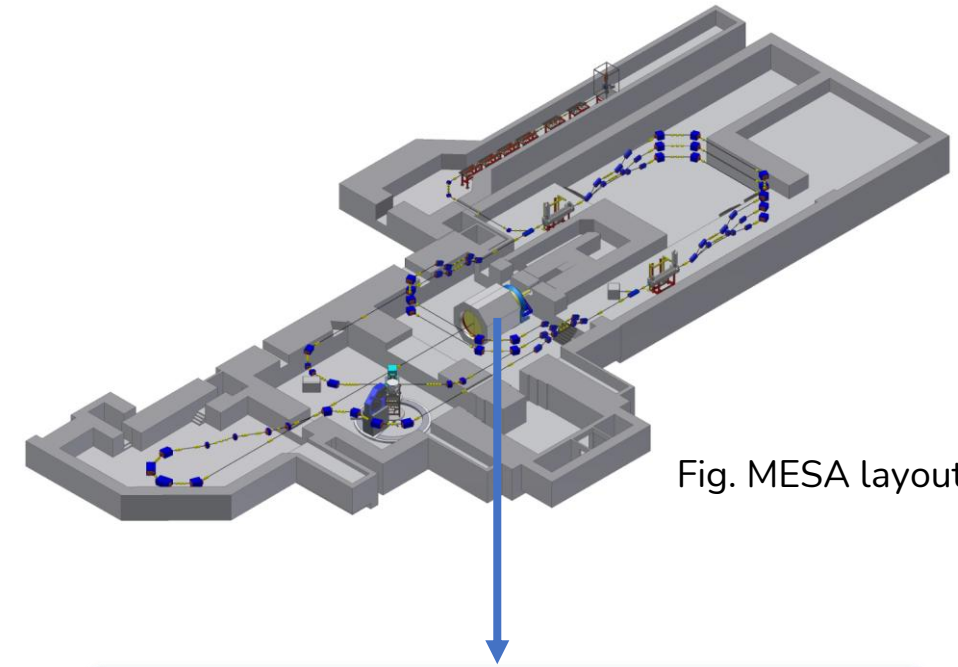


Fig. MESA layout

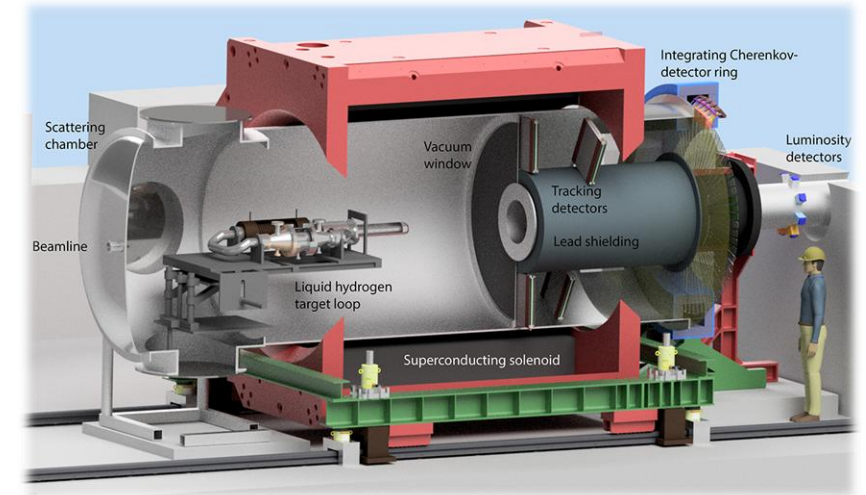


Fig. P2/MREX experiment set-up

Outline for MREX experiment

Mainz Energy-recovering Superconducting Accelerator (MESA):

- 150 μA polarized electron beam with $E_{\text{kin}} = 155 \text{ MeV}$
- Polarization measurement with $<1\%$ uncertainty

P2 experiment:

- High-precision measurement of $\sin^2\theta_W$
- Exchange hydrogen with ^{208}Pb for MREX

MREX vs PREX:

- Same momentum transfer $Q^2 = 0.0062 \text{ (GeV/c)}^2$ to match kinematics and maximize sensitivity to NS
- Solenoid instead of spectrometer geometry

$$Q^2 = -q^2 = -(p - p')^2 = \frac{4EE'}{c^2} \cdot \sin^2\left(\frac{\theta}{2}\right)$$

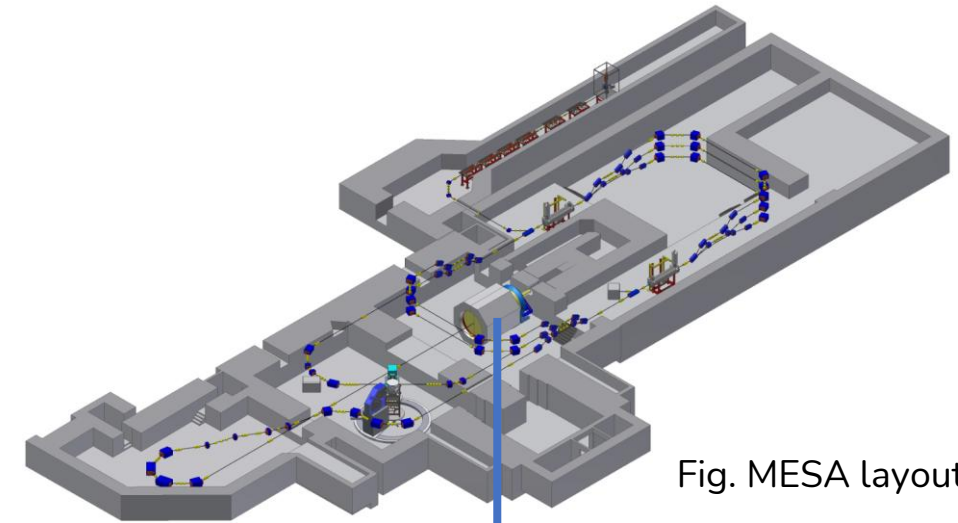
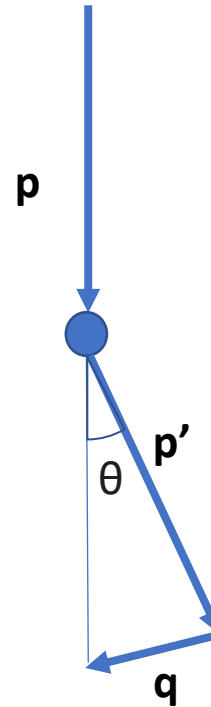


Fig. MESA layout

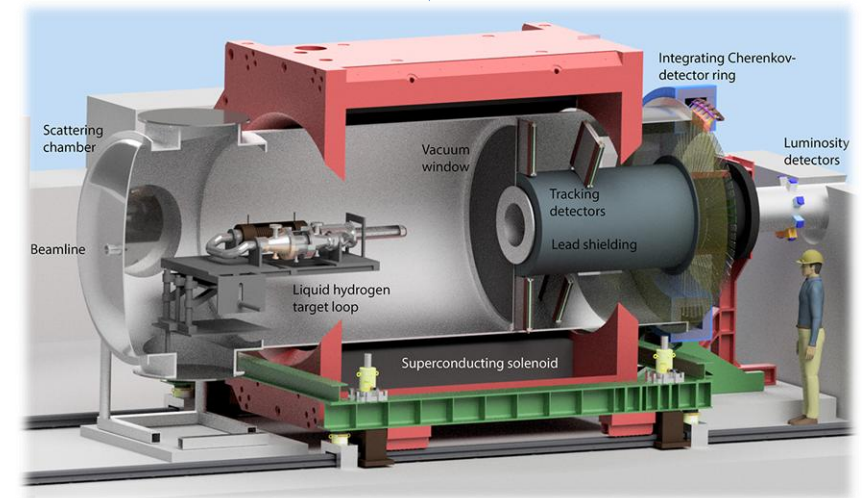


Fig. P2/MREX experiment set-up

Monte-Carlo simulation framework

- Initially created for P2
- Geant4 framework
- Energy deposition
- Multiple scattering
- Secondary particles
- Detector response

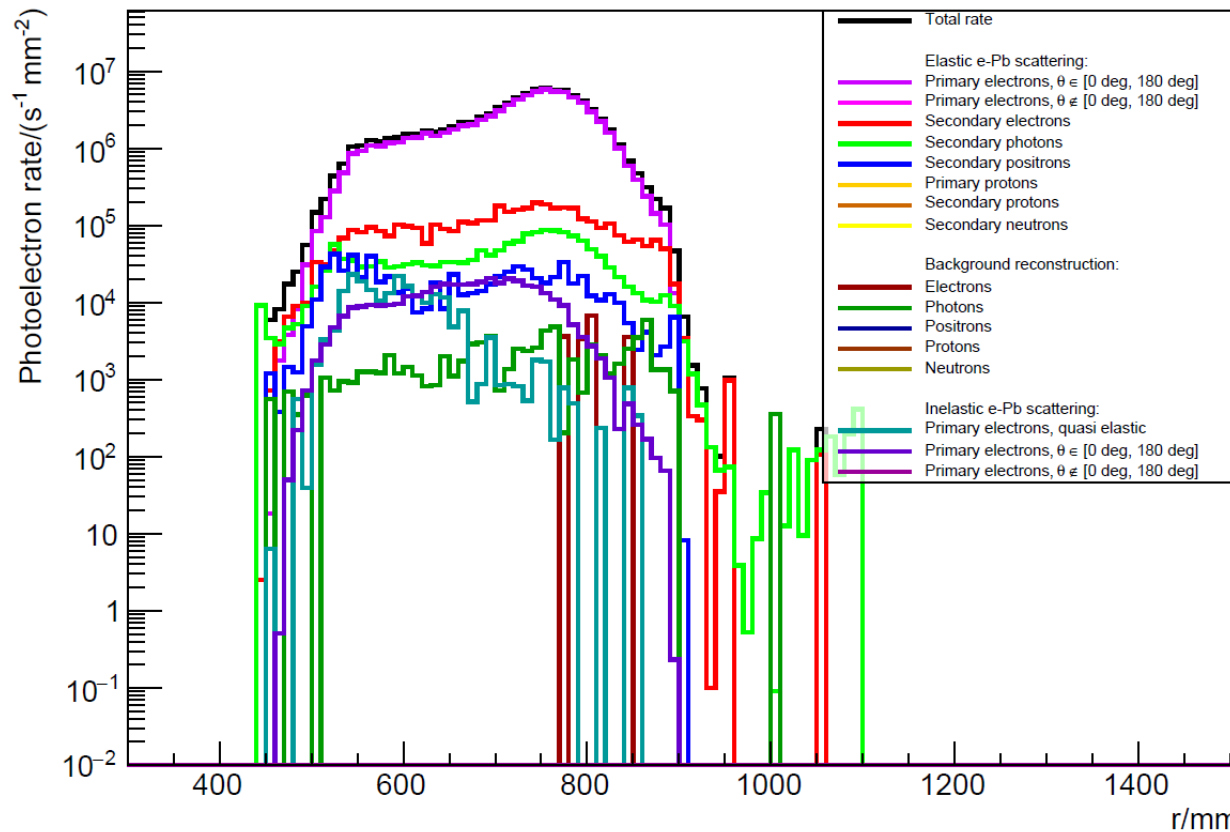
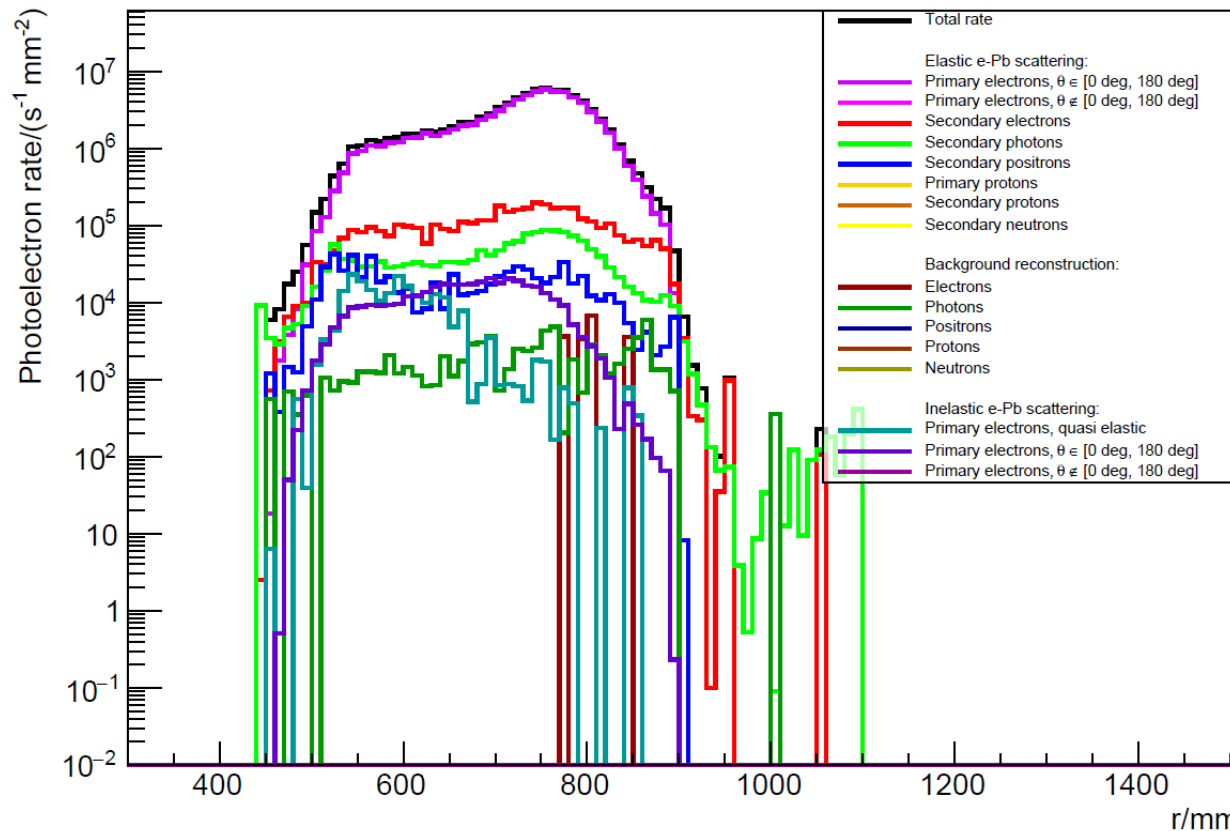


Fig. Radial dependence of the photoelectron rate in Cherenkov detector from different particles

Monte-Carlo simulation framework

- Initially created for P2
- Geant4 framework
- Energy deposition
- Multiple scattering
- Secondary particles
- Detector response
- Inelastic scattering generator
- Additional shielding



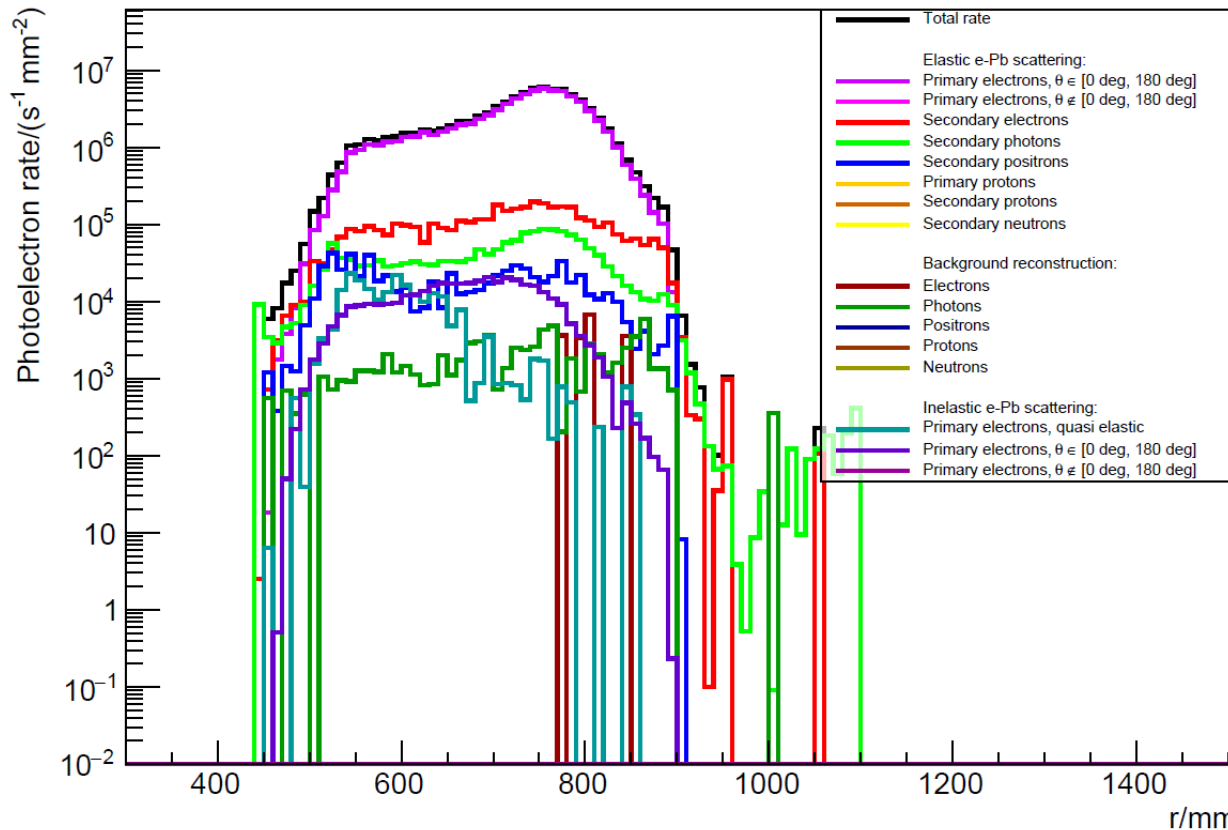
$$A^{meas} = (1 - \sum f_i)A^{el} + \sum f_i A_i, \text{ or}$$

$$A^{el} = \frac{A^{meas} - \sum f_i A_i}{(1 - \sum f_i)}.$$

Fig. Radial dependence of the photoelectron rate in Cherenkov detector from different particles

Monte-Carlo simulation framework

- Initially created for P2
- Geant4 framework
- Energy deposition
- Multiple scattering
- Secondary particles
- Detector response
- Inelastic scattering generator
- Additional shielding
- Systematic and statistical uncertainty



$$A^{meas} = (1 - \sum f_i)A^{el} + \sum f_i A_i, \text{ or}$$

$$A^{el} = \frac{A^{meas} - \sum f_i A_i}{(1 - \sum f_i)}.$$

2.31 ppb (0.37%)

No extra shielding

+1% of syst and
stat from simulation

1.55 ppb (0.25%)

With extra shielding

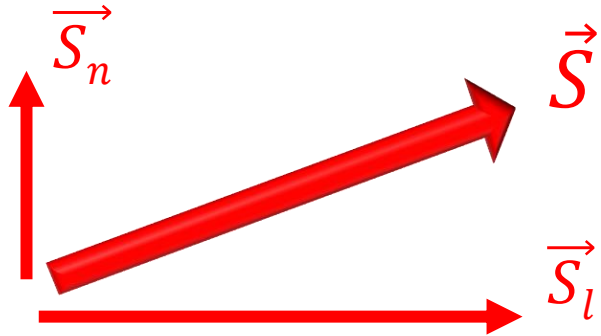


Time, h	$\Delta A_{stat}/A$	Time, h	$\Delta A_{stat}/A$
2300	0.36%	1500	0.48%

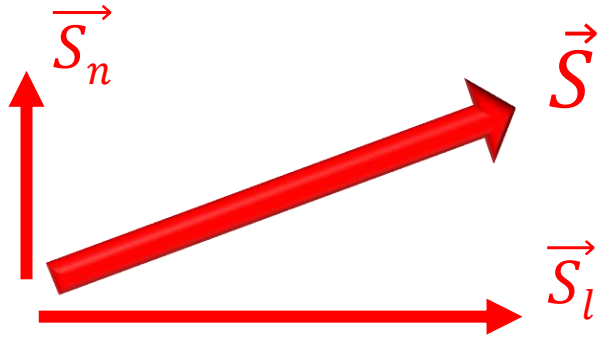
To reach the goal of 0.5% in R_n

Fig. Radial dependence of the photoelectron rate in Cherenkov detector from different particles

Beam-normal single spin asymmetry

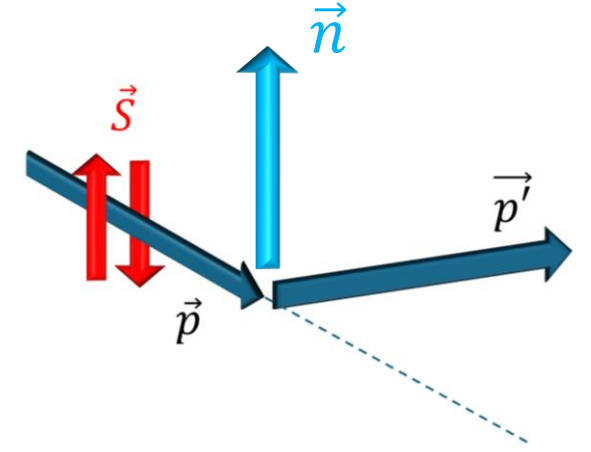


Beam-normal single spin asymmetry

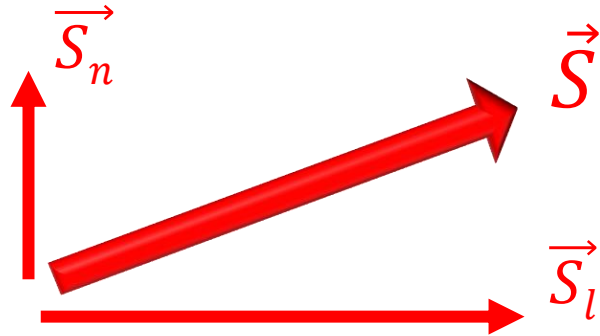


$$A_n = \frac{\sigma^\uparrow - \sigma^\downarrow}{\sigma^\uparrow + \sigma^\downarrow}$$

σ_\uparrow and σ_\downarrow correspond to spins parallel or antiparallel to $\vec{n} = (\vec{p} \times \vec{p}') / |\vec{p} \times \vec{p}'|$

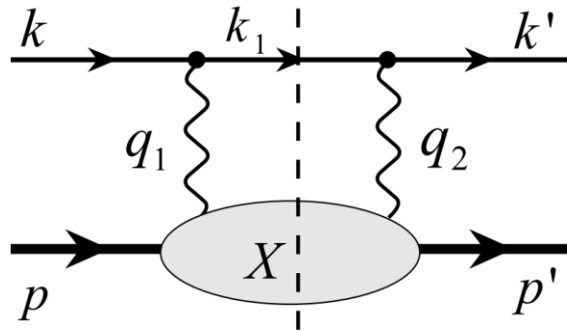
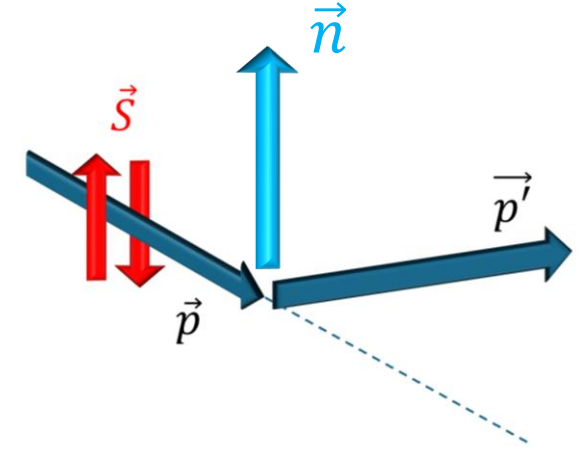


Beam-normal single spin asymmetry



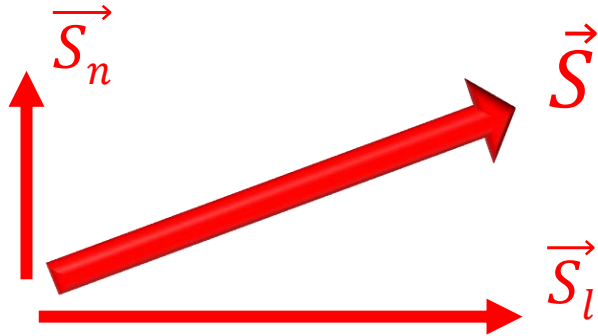
$$A_n = \frac{\sigma^\uparrow - \sigma^\downarrow}{\sigma^\uparrow + \sigma^\downarrow}$$

σ_\uparrow and σ_\downarrow correspond to spins parallel or antiparallel to $\vec{n} = (\vec{p} \times \vec{p}') / |\vec{p} \times \vec{p}'|$



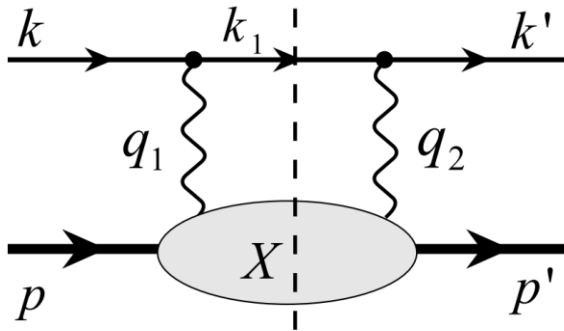
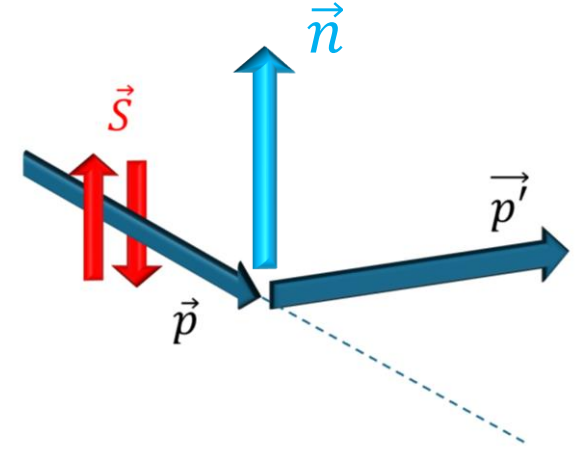
- In leading order arises from interference between one- and two-photon exchange (TPE) amplitudes
- Hard to calculate theoretically because of intermediate inelastic states and multi-photon effects

Beam-normal single spin asymmetry



$$A_n = \frac{\sigma^\uparrow - \sigma^\downarrow}{\sigma^\uparrow + \sigma^\downarrow}$$

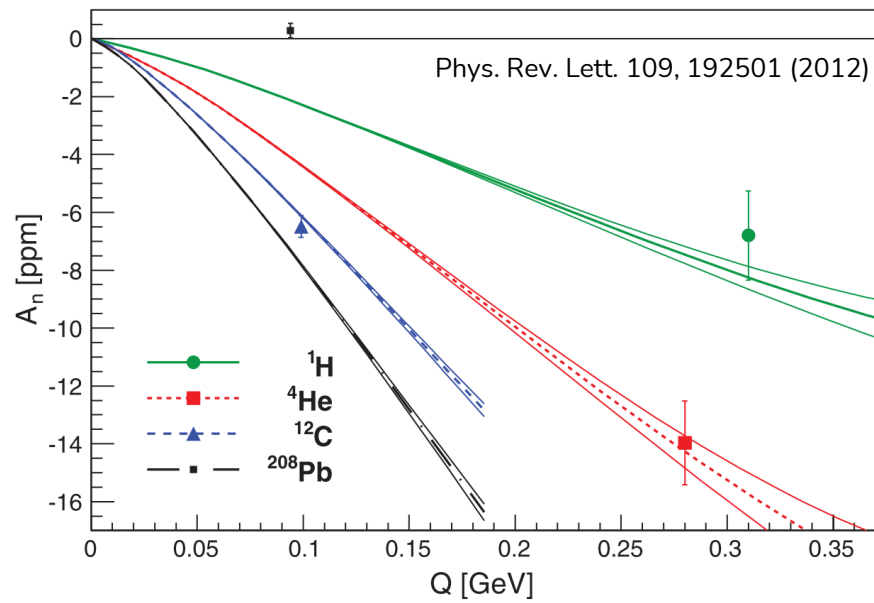
σ_\uparrow and σ_\downarrow correspond to spins parallel or antiparallel to $\vec{n} = (\vec{p} \times \vec{p}') / |\vec{p} \times \vec{p}'|$



- In leading order arises from interference between one- and two-photon exchange (TPE) amplitudes
- Hard to calculate theoretically because of intermediate inelastic states and multi-photon effects

- Much larger than A_{PV} , so can be a source of significant false asymmetry in PVeS
- Significant contribution to radiative corrections in PVeS
- Gives access to TPE - important for proton form factor puzzle and muonic atom spectroscopy

Previous A_n results



Previous A_n results

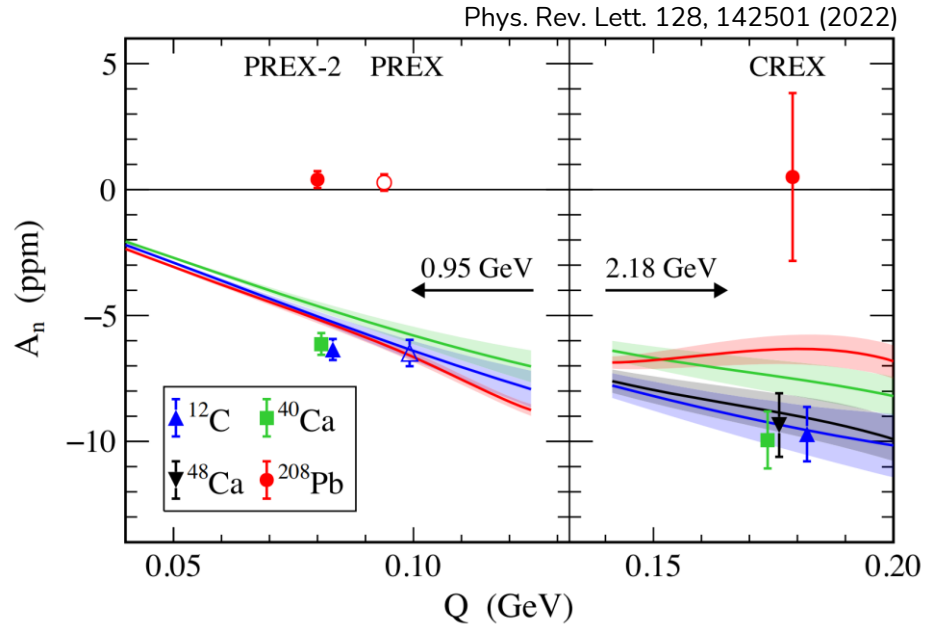
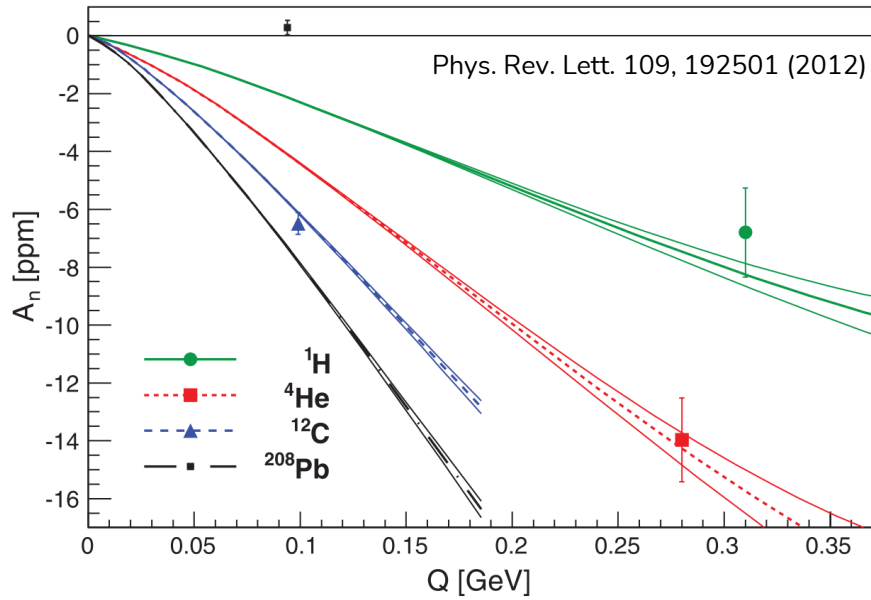


Fig. A_n measurements from HAPPEX, PREX, PREX-2 and CREX for different nuclei with corresponding theoretical predictions

Experiments show vanishing A_n for ^{208}Pb , contradicting theory

Previous A_n results

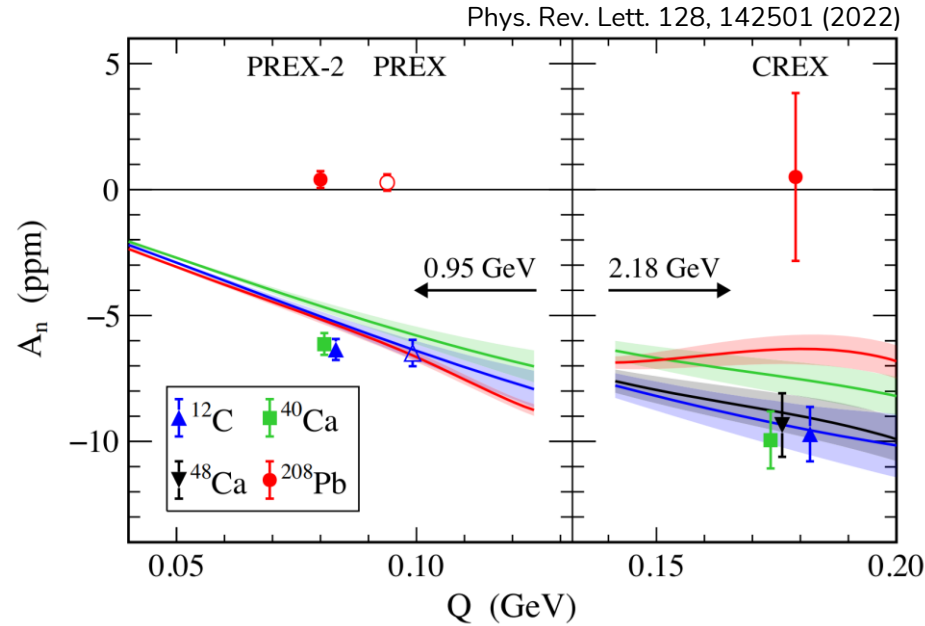
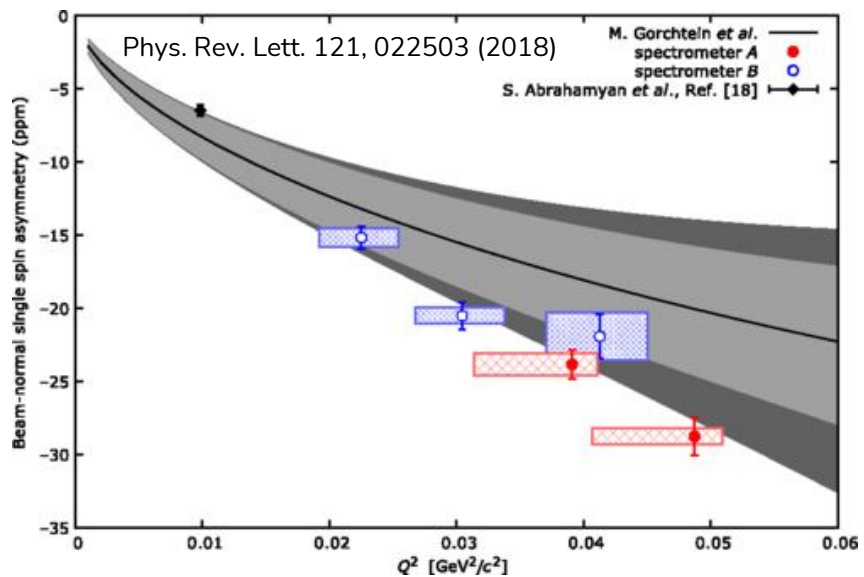
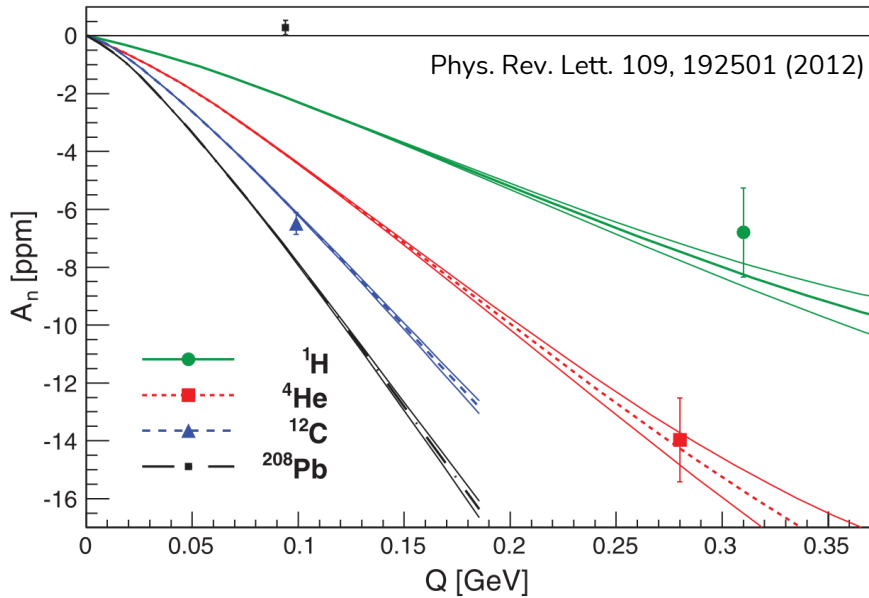


Fig. A_n measurements from HAPPEX, PREX, PREX-2 and CREX for different nuclei with corresponding theoretical predictions

Experiments show vanishing A_n for ^{208}Pb , contradicting theory

Fig. A_n measurements from A1 for different nuclei and Q^2 with corresponding theoretical predictions

Systematic A_n study at the A1 experiment @ MAMI:

- Q^2 dependence of A_n for ^{12}C

Previous A_n results

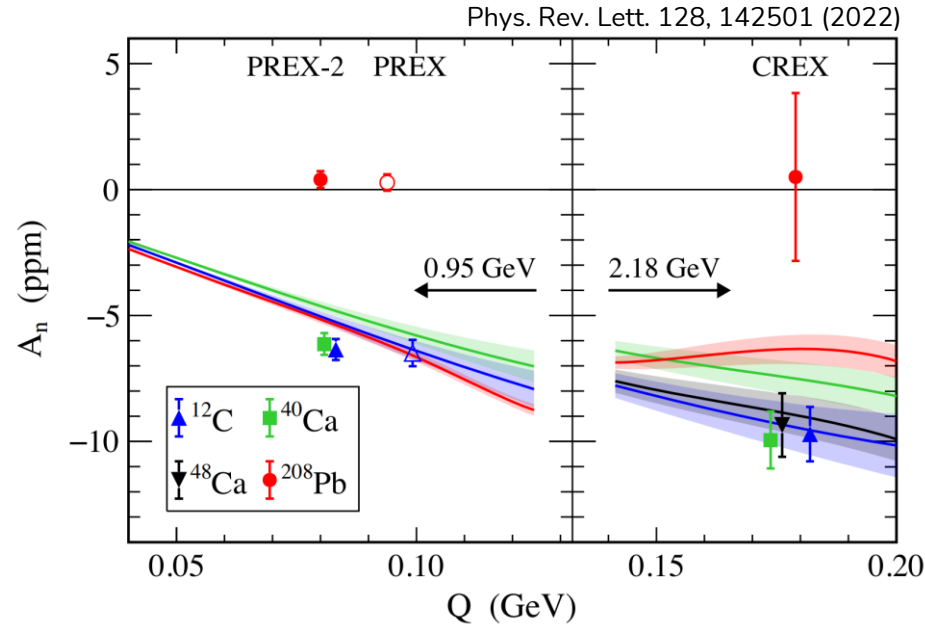
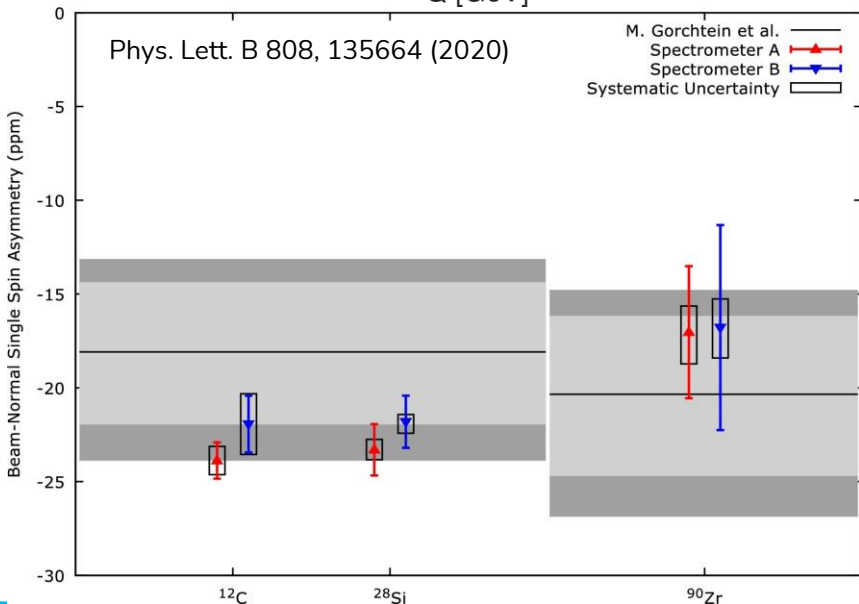
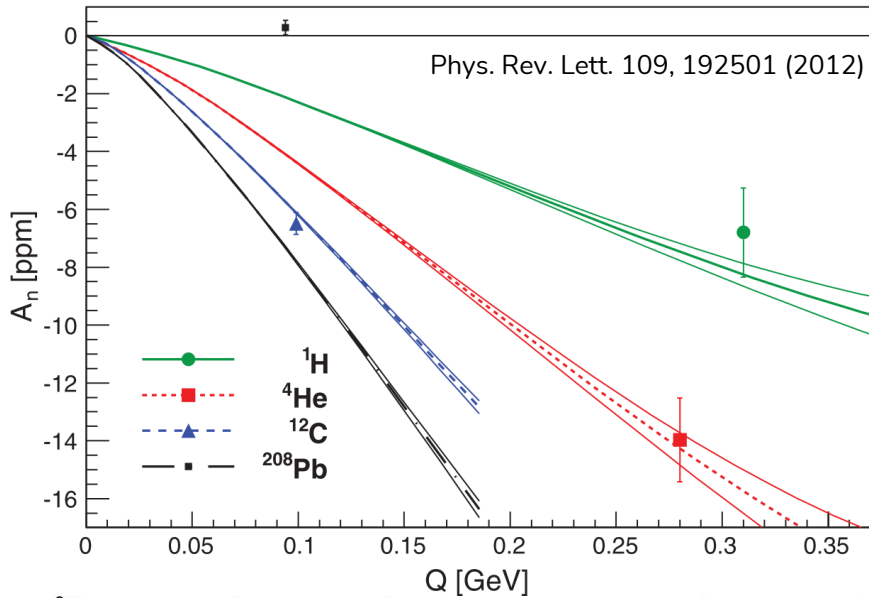


Fig. A_n measurements from A1 for different nuclei and Q^2 with corresponding theoretical predictions

Systematic A_n study at the A1 experiment @ MAMI:

- Q^2 dependence of A_n for ^{12}C
- Z dependance (^{12}C , ^{28}Si , ^{90}Zr) of A_n at the same Q^2

Consistent with theory within uncertainty

Fig. A_n measurements from HAPPEX, PREX, PREX-2 and CREX for different nuclei with corresponding theoretical predictions

Experiments show vanishing A_n for ^{208}Pb , contradicting theory

A_n in electron- ^{208}Pb scattering at Mainz

- 570 MeV 20 μA polarized beam on 0.5 mm cooled ^{208}Pb target

A_n in electron- ^{208}Pb scattering at Mainz

- 570 MeV $20\mu\text{A}$ polarized beam on 0.5 mm cooled ^{208}Pb target
- A and B spectrometers at A1 positioned at $Q^2 \approx 0.04 (\text{GeV}/c)^2$



Fig. View of the A1 spectrometer hall

A_n in electron- ^{208}Pb scattering at Mainz

- 570 MeV $20\mu\text{A}$ polarized beam on 0.5 mm cooled ^{208}Pb target
- A and B spectrometers at A1 positioned at $Q^2 \approx 0.04 (\text{GeV}/c)^2$
- Fused-silica Cherenkov detectors with multiple PMTs at focal plane



Fig. View of the A1 spectrometer hall

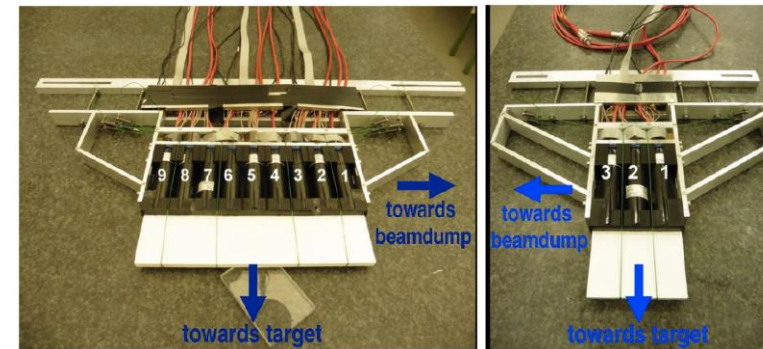


Fig. Fused-silica Cherenkov detectors

A_n in electron- ^{208}Pb scattering at Mainz

- 570 MeV 20 μA polarized beam on 0.5 mm cooled ^{208}Pb target
- A and B spectrometers at A1 positioned at $Q^2 \approx 0.04$ (GeV/c) 2
- Fused-silica Cherenkov detectors with multiple PMTs at focal plane
- Custom DAQ for asymmetry measurement at low rates¹



Fig. View of the A1 spectrometer hall

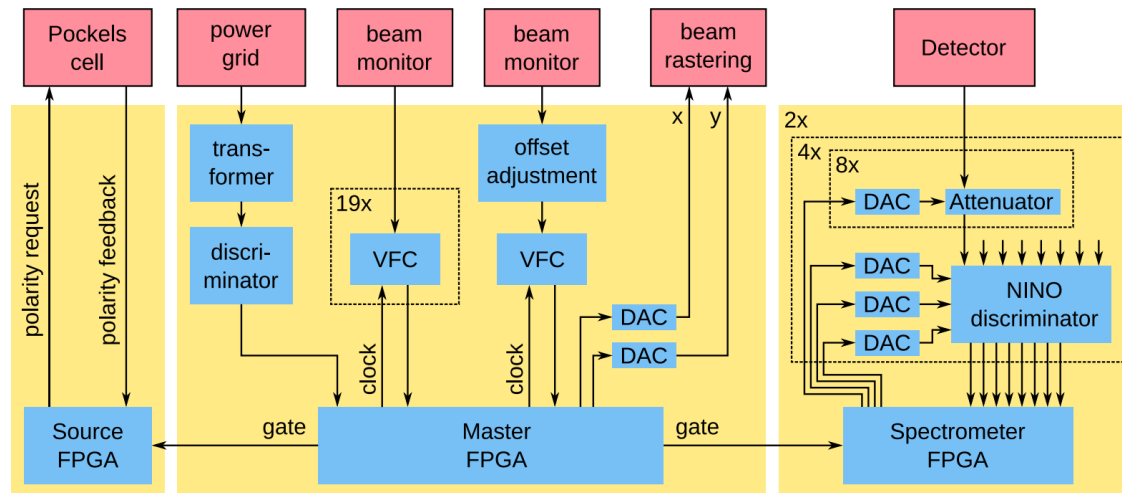


Fig. Sketch of the DAQ system

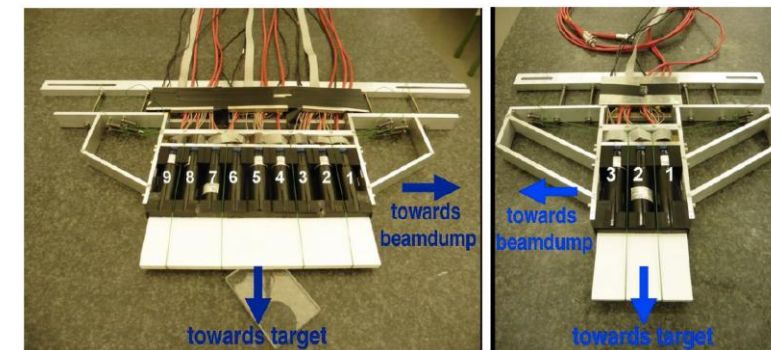


Fig. Fused-silica Cherenkov detectors

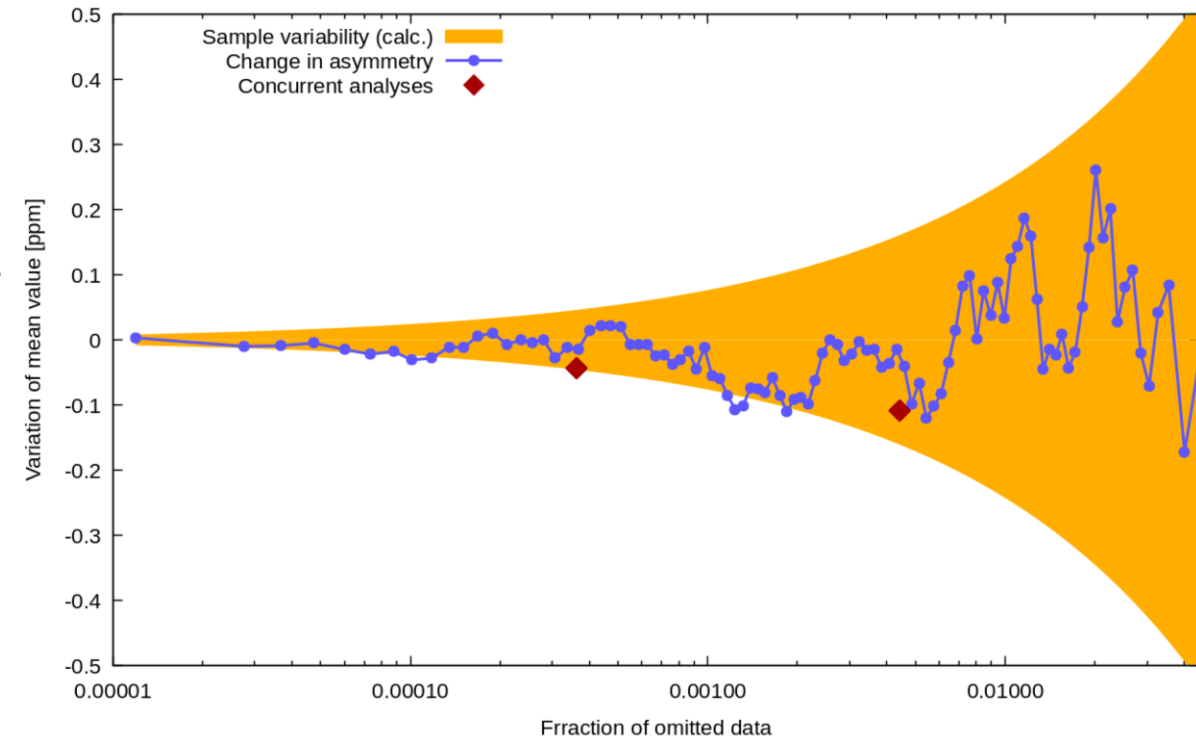
¹ NIM-A 1072, 170187 (2025)

Data analysis

- 232.7 hours of data
- Two separate analysis chains with consistent results
- Manual exclusion of unstabilized beam periods
- Automated quality cuts for individual events

Data analysis

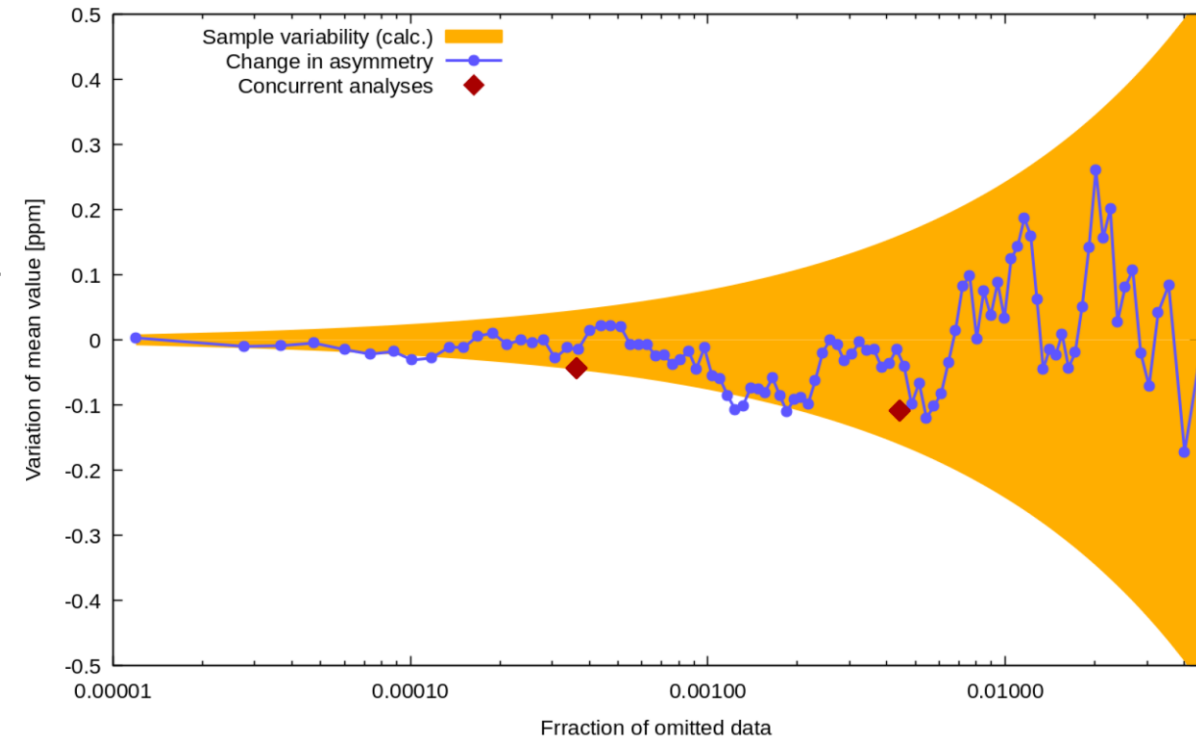
- 232.7 hours of data
- Two separate analysis chains with consistent results
- Manual exclusion of unstabilized beam periods
- Automated quality cuts for individual events



Data analysis

- 232.7 hours of data
- Two separate analysis chains with consistent results
- Manual exclusion of unstabilized beam periods
- Automated quality cuts for individual events

$$A_n = \frac{1}{P_{\perp}} \cdot \left(A_{exp} - c_I A_I - c_X \Delta X - c_Y \Delta Y - c_{X'} \Delta X' - c_{Y'} \Delta Y' - c_E \Delta E \right)$$



Data analysis

- 232.7 hours of data
- Two separate analysis chains with consistent results
- Manual exclusion of unstabilized beam periods
- Automated quality cuts for individual events

$$A_n = \frac{1}{P_{\perp}} \cdot \left(A_{exp} - c_I A_I - c_X \Delta X - c_Y \Delta Y - c_{X'} \Delta X' - c_{Y'} \Delta Y' - c_E \Delta E \right)$$

Spectrometer	A	B
$\Delta(\partial\sigma/\partial x)$	< 0.001	< 0.001
$\Delta(\partial\sigma/\partial y)$	0.012	0.009
$\Delta(\partial\sigma/\partial x')$	< 0.001	0.006
$\Delta(\partial\sigma/\partial y')$	0.012	0.003
$\Delta(\partial\sigma/\partial E)$	0.031	0.018
ΔA_I	0.008	0.008
ΔGain	0.034	0.016
ΔTails	0.145	0.034
$\Delta \text{Inversion}$	0.026	0.074
$\Delta \text{Analysis}$	0.029	0.611
ΔP	0.109	0.117

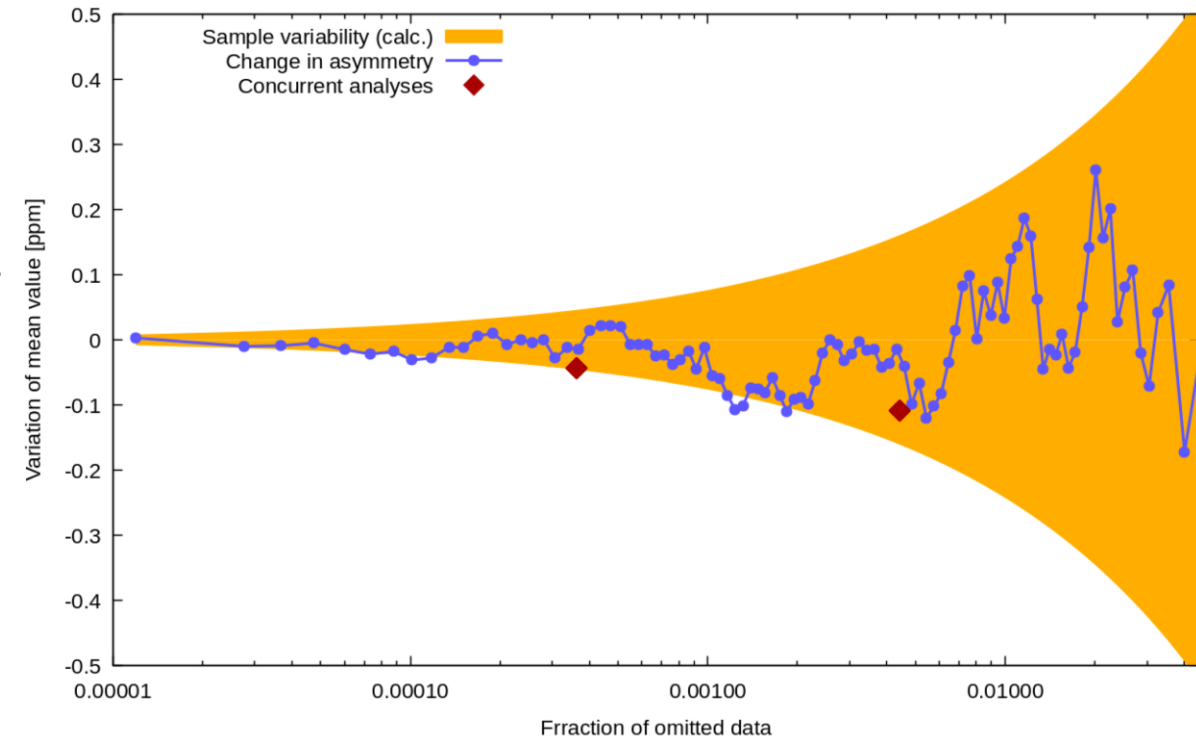
ΔGain - PMT gain variations

ΔTails - shift in asymmetry from exclusion of 0.1% outliers

$\Delta \text{Inversion}$ - from different number of events with GVZ in and out

$\Delta \text{Analysis}$ - difference between two independent analysis chains

ΔP - uncertainty from polarization measurement



Results

Final value for ^{208}Pb :

$$A_n = -9.1 \pm 2.1_{\text{stat}} \pm 0.7_{\text{syst}} \text{ ppm}$$

[arXiv:2508.18851](https://arxiv.org/abs/2508.18851)

- Different kinematics compared to PREX/CREX, but clear $A_n \neq 0$
- Latest theory fails to reproduce both
- Systematic study needed
- Crucial for MREX

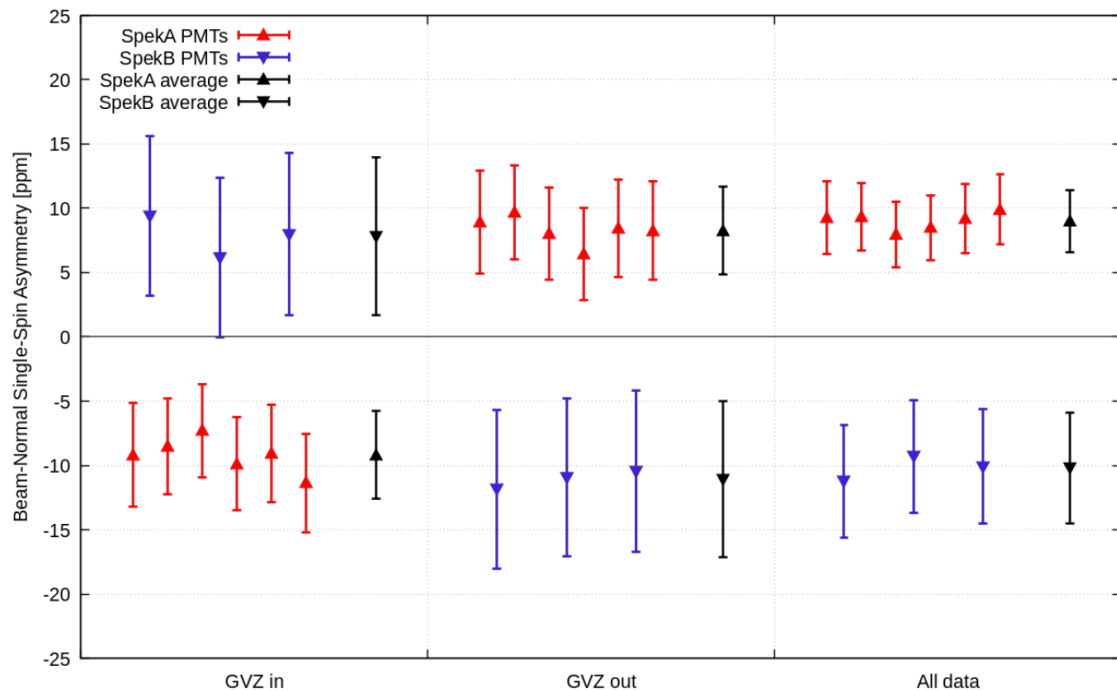


Fig. Measured A_n for different PMTs, spectrometers and GVZ positions

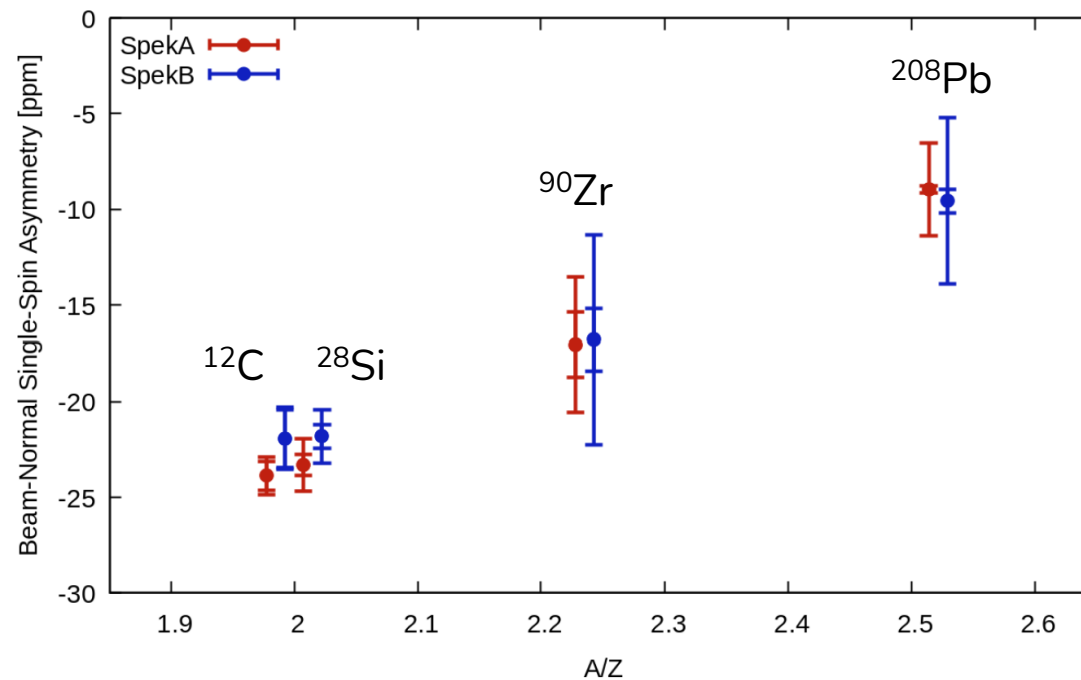


Fig. A_n measured at MAMI for different nuclei at the same Q^2

Summary

- Neutron skin in ^{208}Pb allows to constrain EoS and neutron stars
- PREX measurement should be improved and cross-checked
- Simulations show that 0.5% uncertainty in R_n is reachable for MREX
- Precise knowledge of A_n is important, but theory contradicts $A_n \approx 0$ from the PREX experiment for ^{208}Pb
- Our latest result of $A_n = -9.1 \pm 2.1_{\text{stat}} \pm 0.7_{\text{syst}}$ ppm for ^{208}Pb at $Q^2 = 0.04 \text{ (GeV/c)}^2$ does not confirm vanishing asymmetry
- Further studies are necessary from both theory and experiment side

Thank you for your attention!

Back-up

Why PREX is not enough?

- Slight tension with astrophysics
- Statistical uncertainty must be decreased



Perform another PVES determination and decrease total uncertainty by a factor of 2

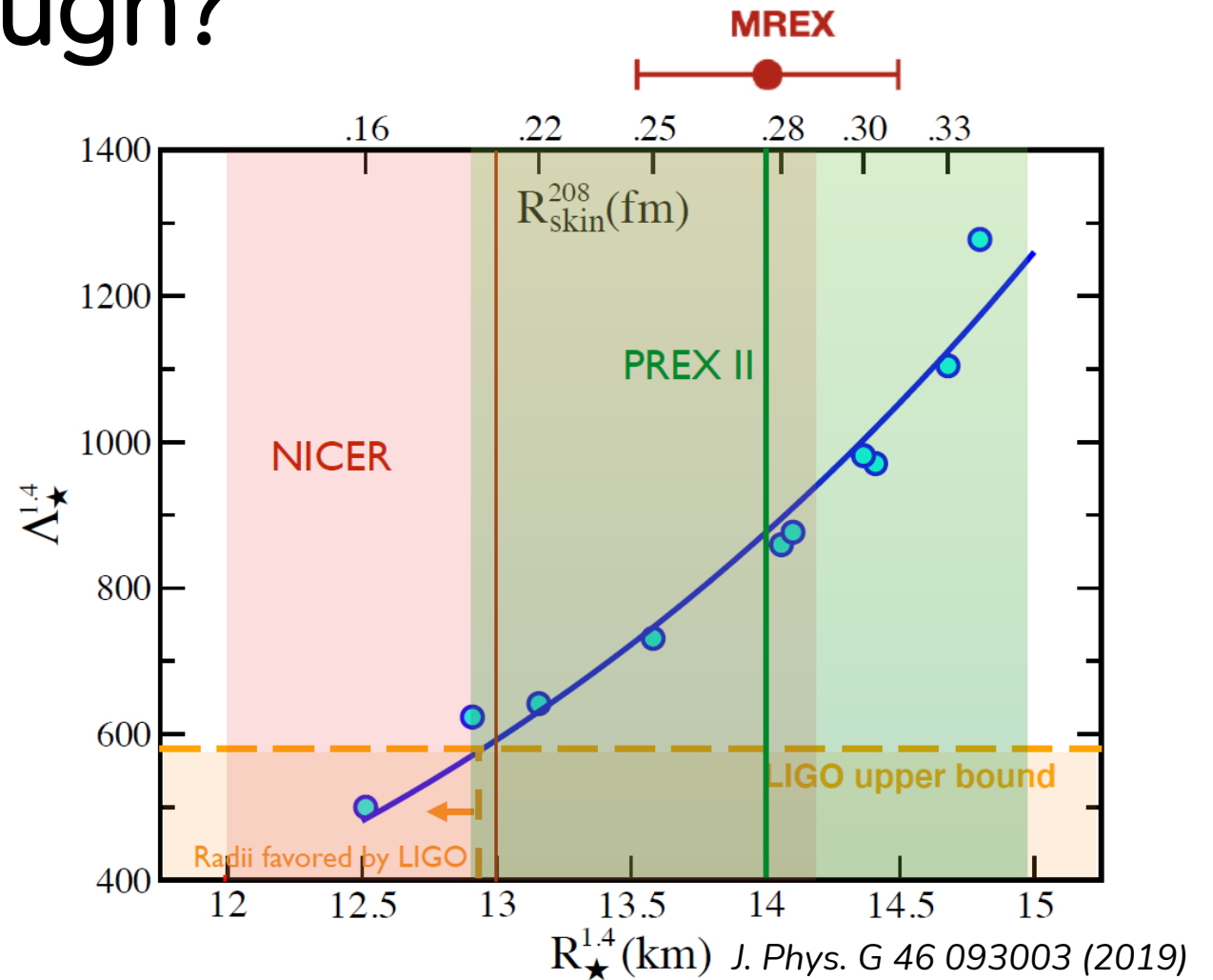


Fig. Connection between neutron skin in ^{208}Pb and astrophysical observables

Outline for MREX

Average momentum transfer of $Q^2 = 0.0062 \text{ (GeV/c)}^2$ to match PREX kinematics and maximize sensitivity to neutron skin

$$Q^2 = -q^2 = -(p - p')^2 = \frac{4EE'}{c^2} \cdot \sin^2\left(\frac{\theta}{2}\right)$$

$$\text{FOM} = \frac{d\sigma}{d\Omega} \times (A^{\text{PV}})^2 \times \varepsilon^2 \quad \varepsilon = \frac{d \ln(A^{\text{PV}})}{d \ln(R_n)} = \frac{R_n}{A^{\text{PV}}} \frac{\delta A^{\text{PV}}}{\delta R_n}$$

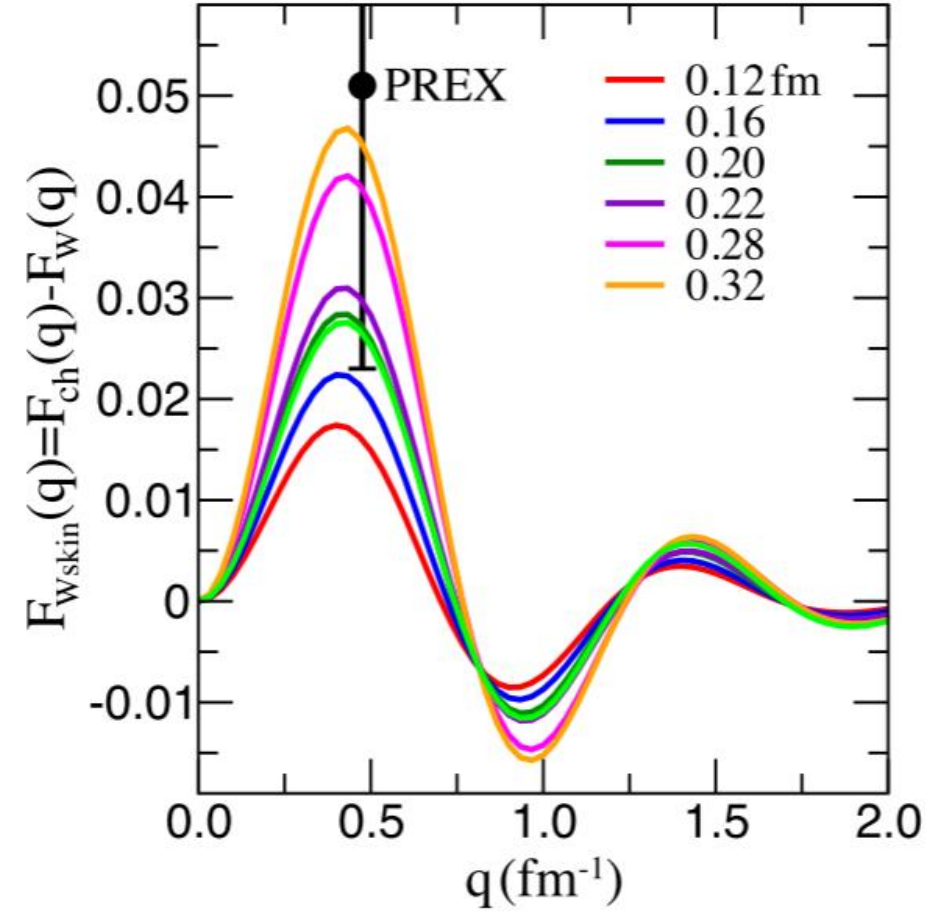
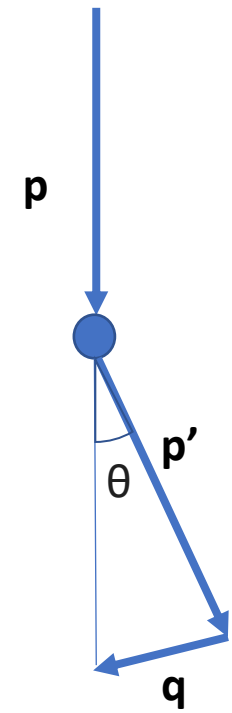
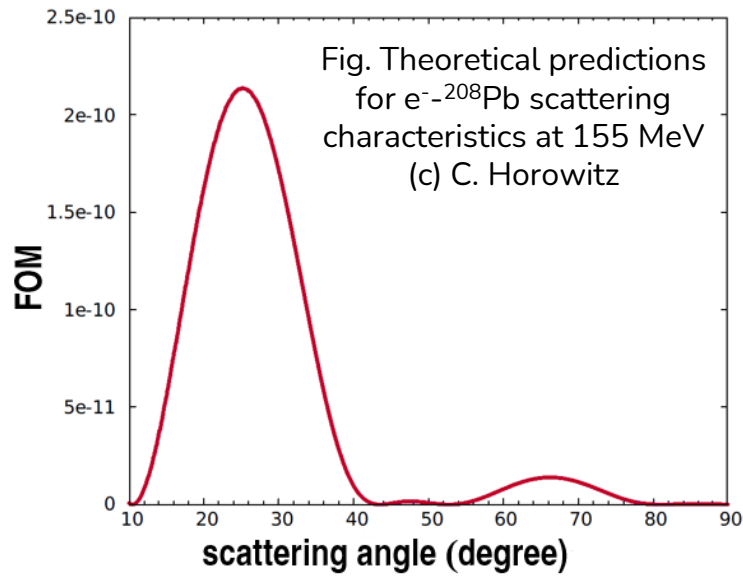


Fig. Theoretical predictions of $F_{\text{ch}} - F_{\text{weak}}$ for ^{208}Pb nuclei with different NS thicknesses

Spectrometer vs solenoid

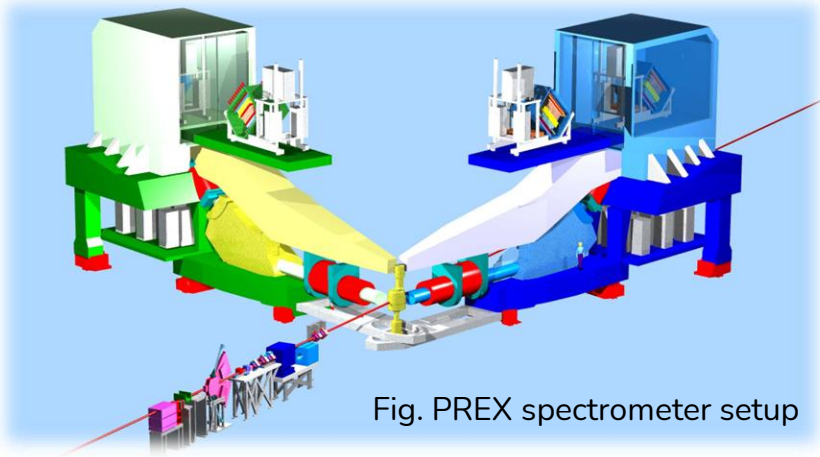


Fig. PREX spectrometer setup

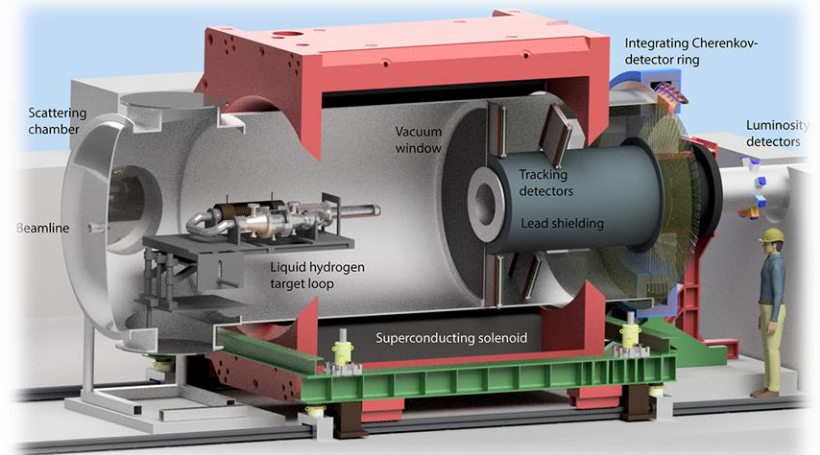


Fig. P2/MREX solenoid set-up

$B = 0.70 \text{ T}$, target center @ $z = -360 \text{ mm}$

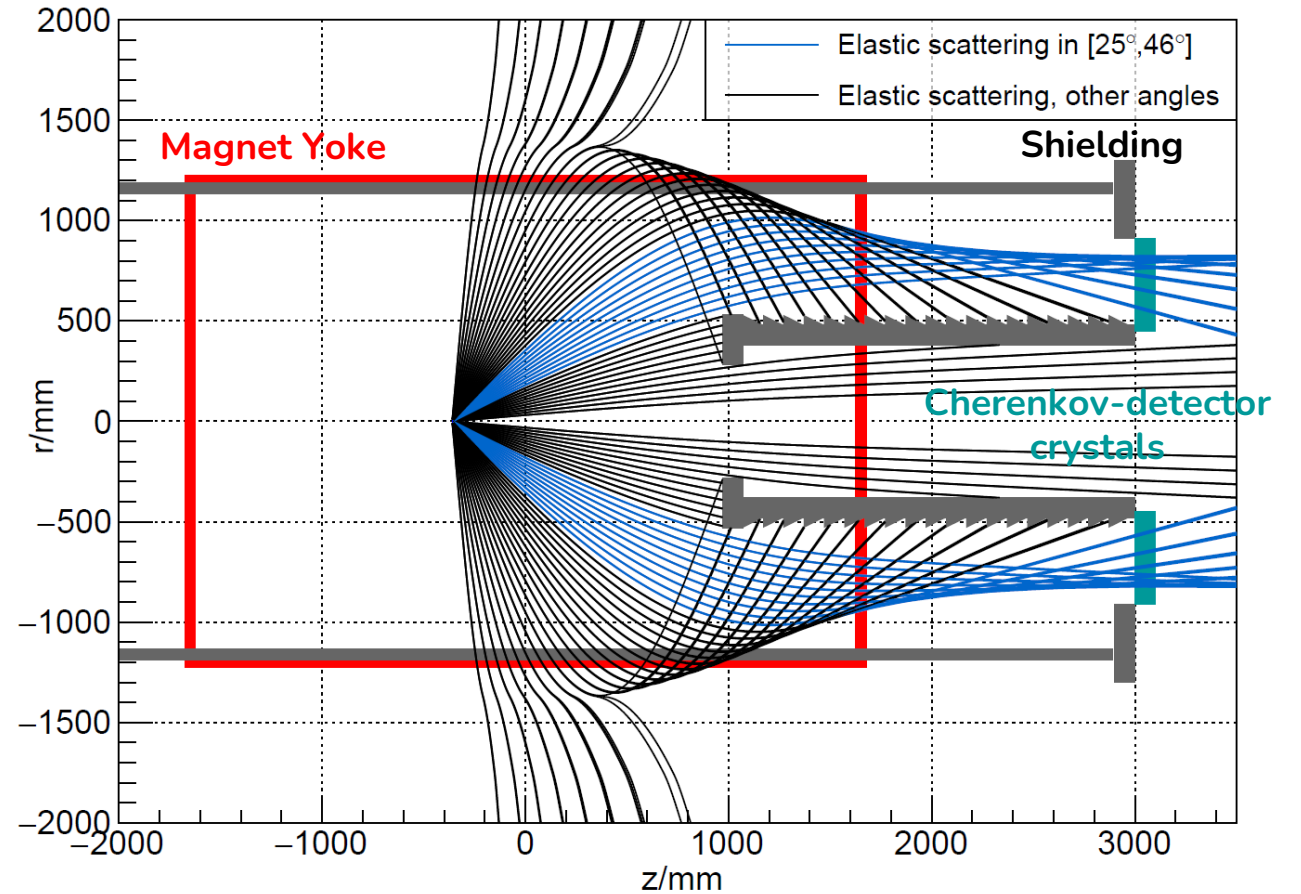


Fig. Tracks of elastically scattered electrons in P2 solenoid

Need to match momentum transfer while maximizing signal from elastic line

Acceptance and measuring time

Assuming additional 1% systematic uncertainty in A^{PV} from beam monitors:

$$\Delta A_{syst} = 1.15\%$$

$$\Delta A_{syst} = 1.12\%$$

Uncertainty in R_n	No extra shielding		With extra shielding	
	Time, h	$\Delta A_{stat}/A$	Time, h	$\Delta A_{stat}/A$
0.5%	2300	0.36%	1500	0.48%

PREX-2 uncertainty: $\Delta A_{stat}/A = 2.9\%$, $\Delta A_{syst}/A = 1.5\%$

Further work:

- Inelastic uncertainty constraint
- Multiple EoS input to get the $A(R_{skin})$ dependence
- Radiation simulation
- Target and shielding development
- Radiative corrections to A_{PV}

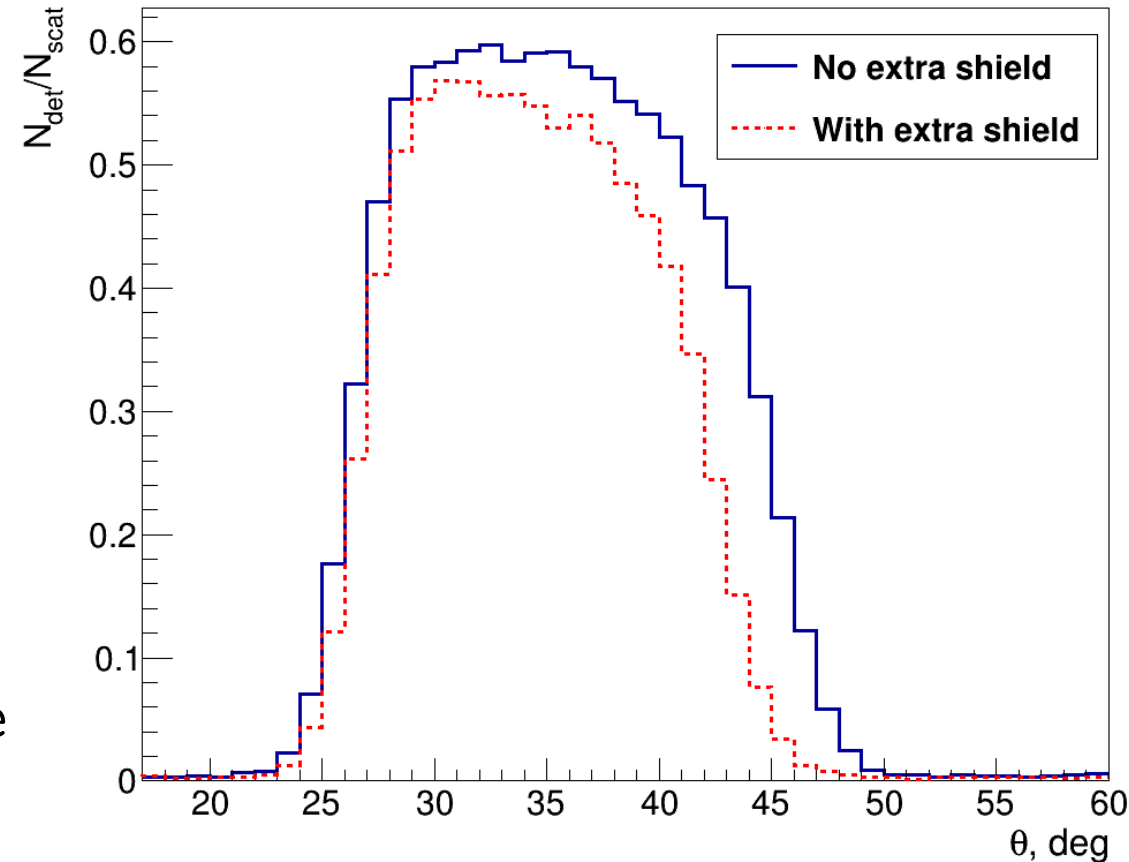
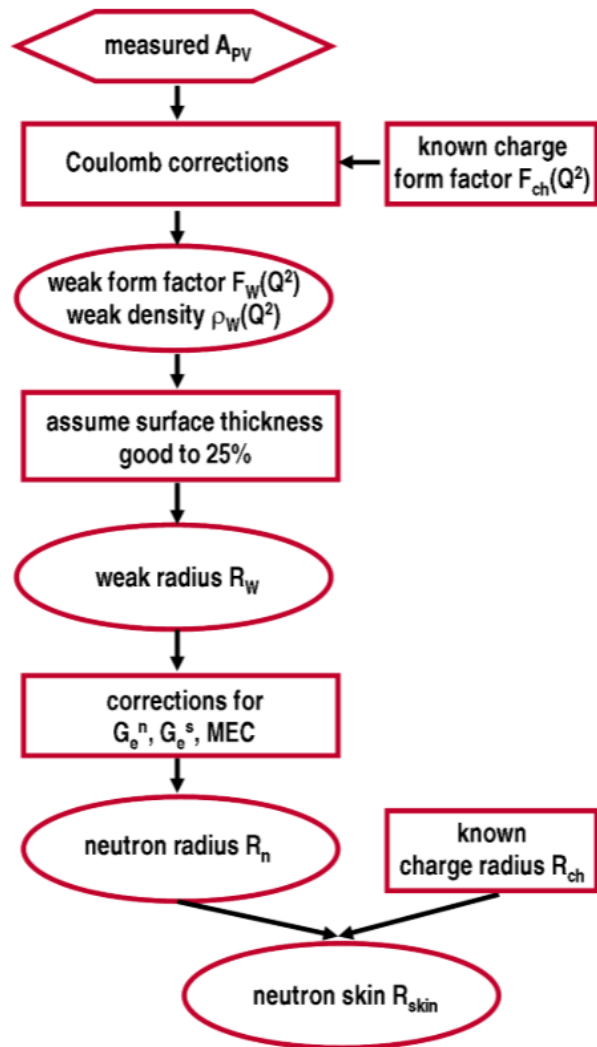


Fig. Fraction of elastically scattered electrons reaching the detector with and without additional shielding

Systematics from theory



Non-elastic systematic play huge part:

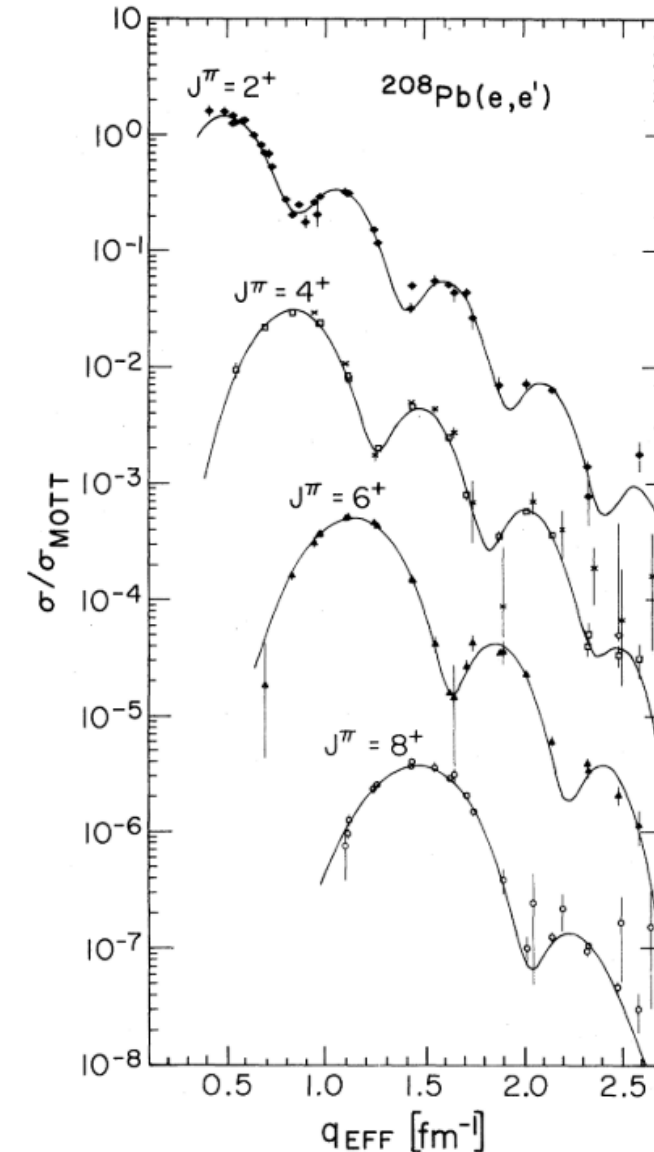
3⁻ and 2⁺ - low-lying excited states
 MR - Multipole resonances
 Other Inel. - other excited states and GDR
 QE - quasielastic scattering
 TGB - target background
 Secondary - secondary produced particles

Contribution i	3 ⁻ and 2 ⁺	MR	Other Inel.	QE	TBG	Secondary
ΔA_i	$0.625 \cdot A_{el}$	$0.625 \cdot A_{el}$	$1.5 \cdot A_{el}$	$2 \cdot A_{QE} $	0	$ A_{el} - A_{Secondary} $
$\Delta f_i/f_i$	20%	50%	100%	100%	10%	10%

Contribution i	No additional shielding			With additional shielding		
	ΔA_i^f , ppb	ΔA_i^A , ppb	ΔA_i , ppb	ΔA_i^f , ppb	ΔA_i^A , ppb	ΔA_i , ppb
Secondary electrons	0.06	0.51	0.51	0.01	0.05	0.05
Secondary photons	0.07	0.62	0.63	0.04	0.34	0.34
Secondary positrons	0.01	0.04	0.04	0.01	0.05	0.05
Target background	0.08	0.18	0.20	0.06	0.15	0.16
3 ⁻ 2.615 MeV	0.10	0.46	0.47	0.07	0.43	0.44
2 ⁺ 4.085 MeV	0.05	0.35	0.36	0.04	0.34	0.34
MR below GDR	0.18	0.52	0.55	0.14	0.49	0.51
Other Inelastic	0.52	0.72	0.88	0.42	0.59	0.73
Quasielastic electrons	1.20	1.34	1.8	0.73	0.80	1.08
Total ΔA_{ne}, ppb	2.31			1.55		

Rates and asymmetries

Contribution i	No additional shielding			With additional shielding		
	R_i , MHz	R_i^{ph} , GHz	A_i , ppb	R_i , MHz	R_i^{ph} , GHz	A_i , ppb
Elastic electrons	$3.64 \cdot 10^4$	$3.61 \cdot 10^3$ (92.18%)	607.61	$2.59 \cdot 10^4$	$2.22 \cdot 10^3$ (89.61%)	608.18
Secondary electrons	$6.17 \cdot 10^3$	$1.74 \cdot 10^2$ (4.45%)	613.07	$5.44 \cdot 10^3$	$1.45 \cdot 10^2$ (5.84%)	618.88
Secondary photons	$7.03 \cdot 10^4$	$6.89 \cdot 10^1$ (1.76%)	599.09	$6.54 \cdot 10^4$	$5.67 \cdot 10^1$ (2.28%)	622.29
Secondary positrons	$5.16 \cdot 10^2$	$3.06 \cdot 10^3$ (0.78%)	613.28	$6.34 \cdot 10^2$	$3.48 \cdot 10^2$ (1.40%)	627.88
Secondary neutrons	$1.20 \cdot 10^3$	0 (0%)	0	$1.26 \cdot 10^3$	0 (0%)	0
Target photons	$4.96 \cdot 10^5$	$3.15 \cdot 10^0$ (0.08%)	0	$5.04 \cdot 10^5$	$2.73 \cdot 10^0$ (0.11%)	0
Other TBG	$1.74 \cdot 10^4$	$4.41 \cdot 10^0$ (0.13%)	0	$1.83 \cdot 10^4$	$1.03 \cdot 10^1$ (0.42%)	0
3^- 2.615 MeV	$5.24 \cdot 10^1$	$4.49 \cdot 10^0$ (0.15%)	943.80	$3.30 \cdot 10^1$	$2.42 \cdot 10^0$ (0.10%)	879.61
2^+ 4.085 MeV	$4.12 \cdot 10^1$	$3.72 \cdot 10^0$ (0.09%)	861.60	$2.67 \cdot 10^1$	$2.06 \cdot 10^0$ (0.08%)	806.96
MR below GDR	$6.21 \cdot 10^1$	$5.33 \cdot 10^0$ (0.14%)	854.77	$2.43 \cdot 10^1$	$1.82 \cdot 10^0$ (0.07%)	772.56
Other Inelastic	$2.88 \cdot 10^1$	$2.42 \cdot 10^0$ (0.06%)	0	$1.37 \cdot 10^1$	$1.02 \cdot 10^0$ (0.04%)	0
Quasielastic electrons	$1.11 \cdot 10^2$	$9.00 \cdot 10^0$ (0.23%)	608.18	$1.32 \cdot 10^1$	$1.04 \cdot 10^0$ (0.04%)	-51.86
Total	$6.28 \cdot 10^5$	$3.92 \cdot 10^3$ (100%)	608.71	$6.21 \cdot 10^5$	$2.48 \cdot 10^3$ (100%)	608.35

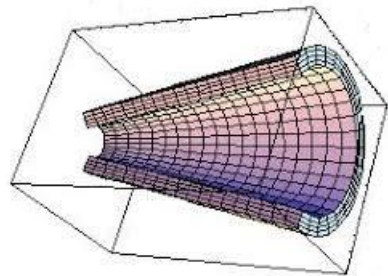


Additional shielding to reduce inelastic

- Need a way to reduce uncertainty from inelastic contribution
- Moving target upstream can help, but need to stick to the same Q^2



Additional conical shielding next to target



$B = 0.70$ T, target center @ $z = -550$ mm

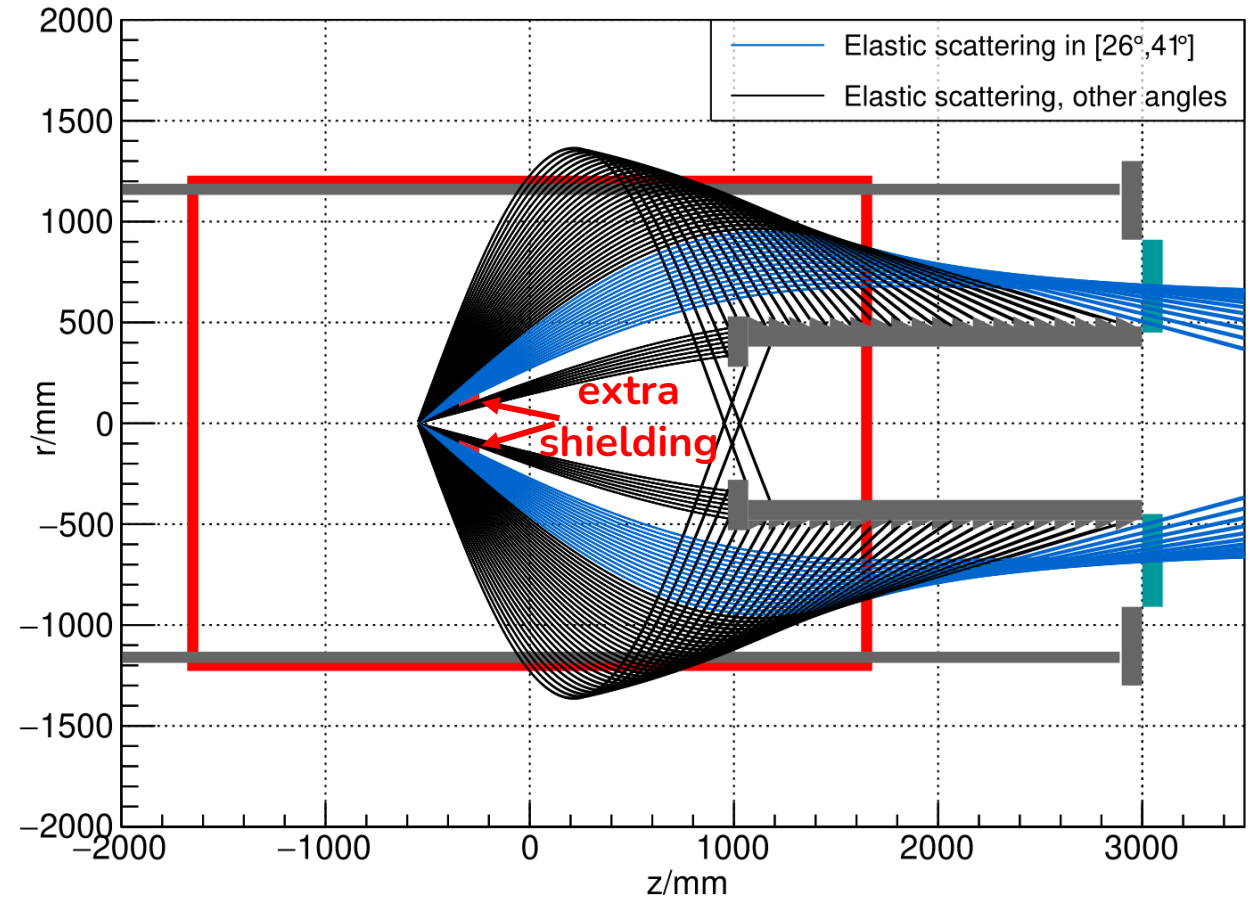
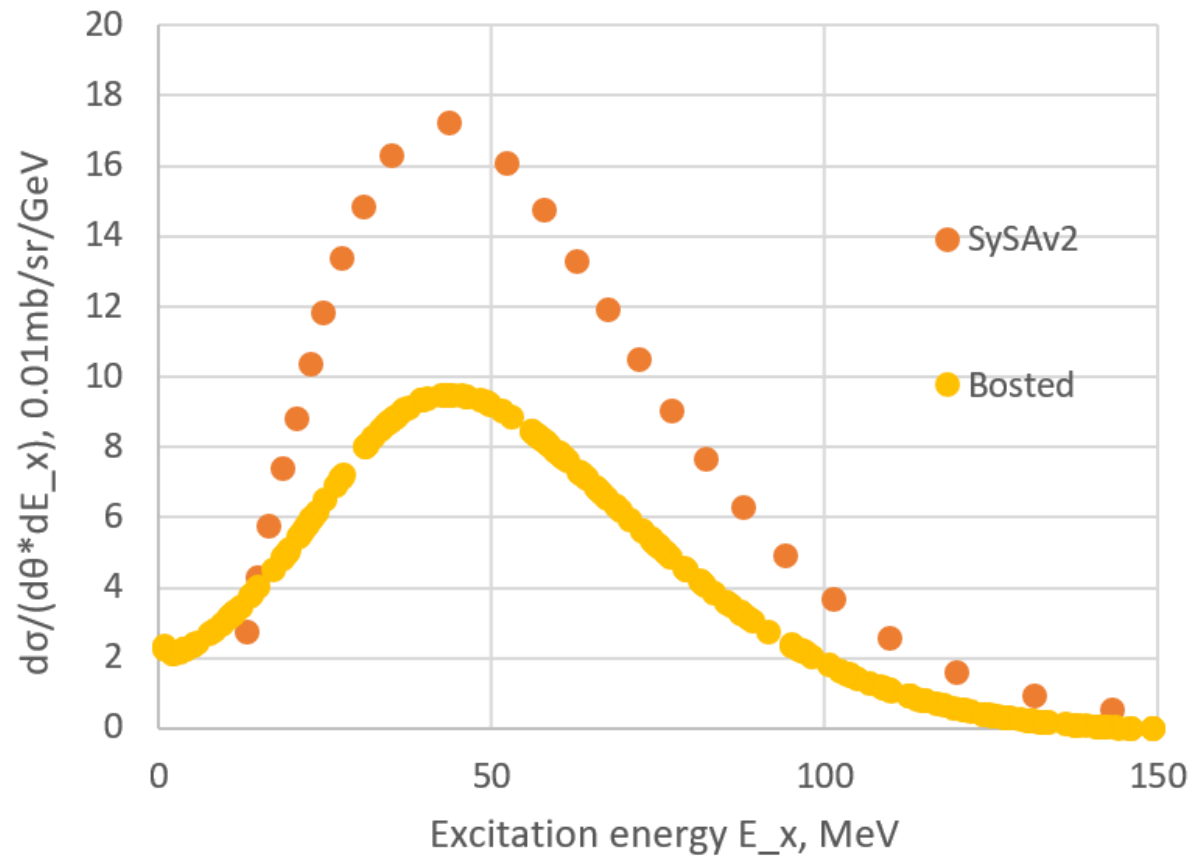


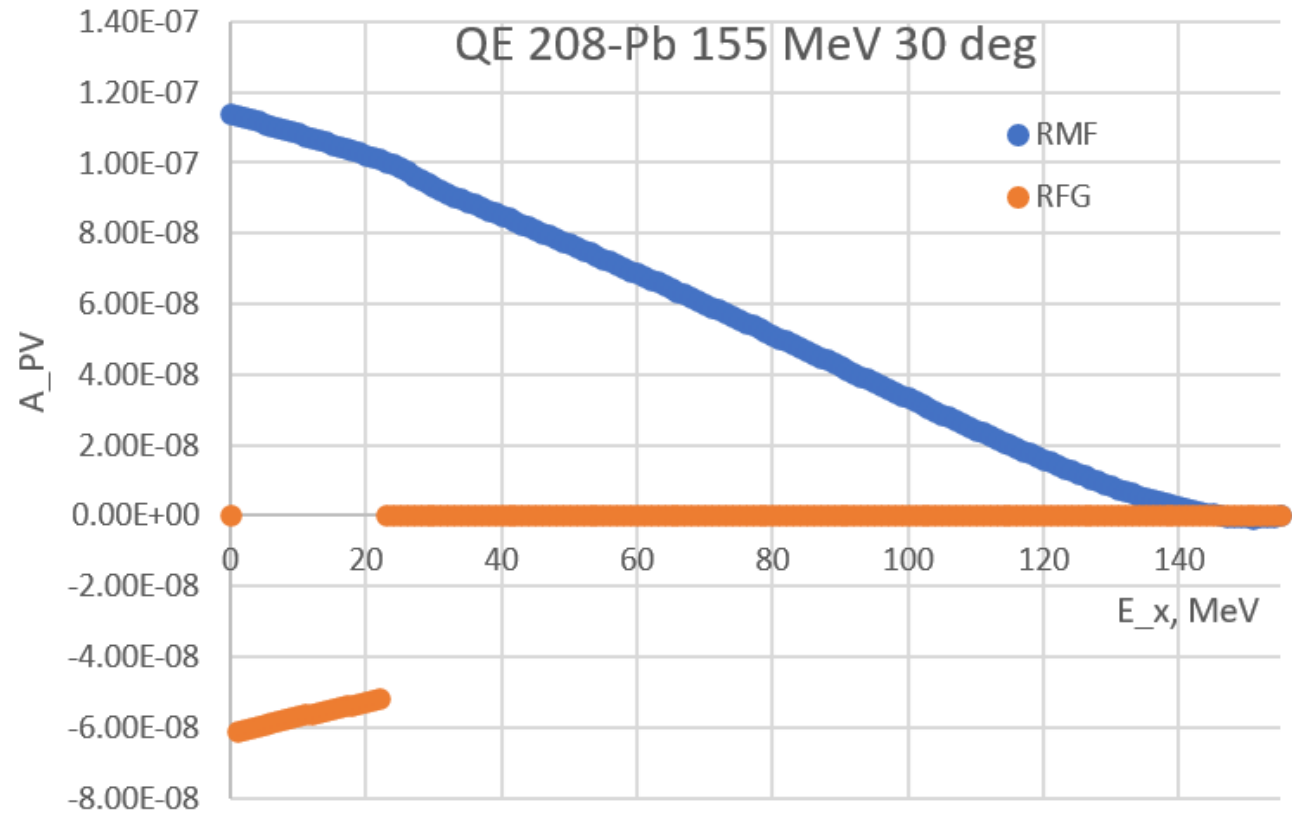
Fig. Tracks of elastically scattered electrons in P2 solenoid with additional shielding

Quasielastic scattering

C-12, E = 400 MeV, $\theta = 36$ deg

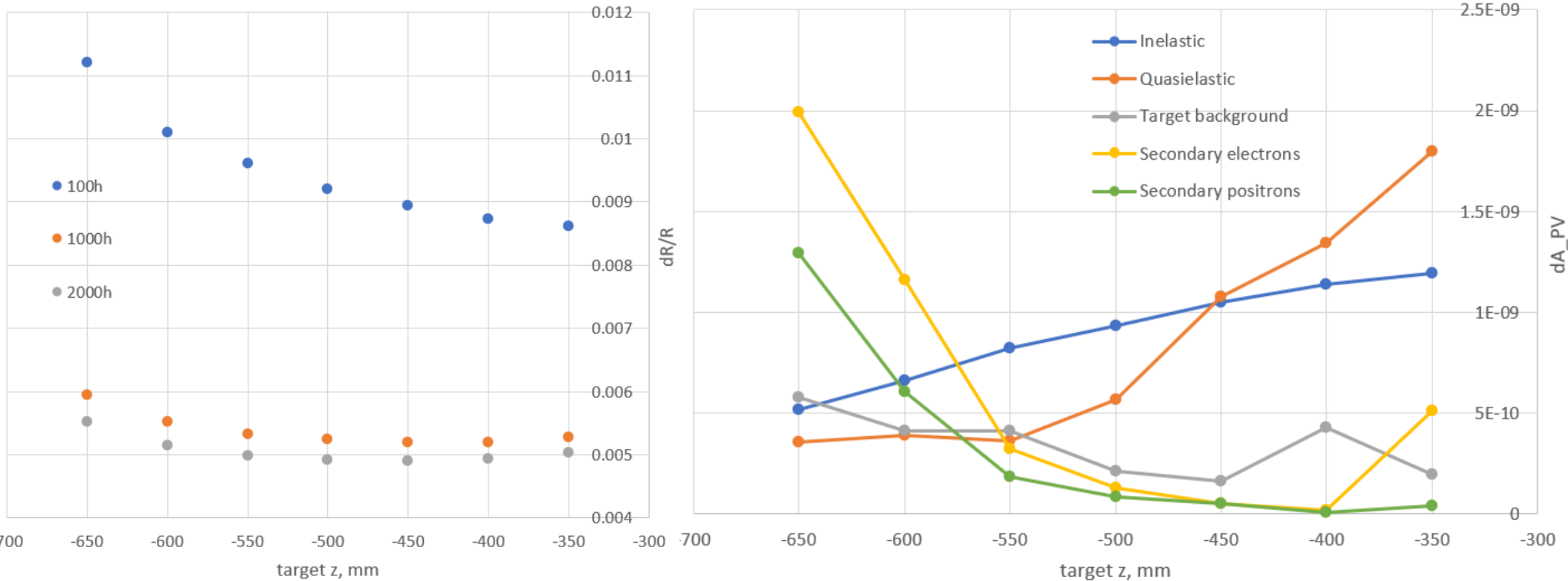


Cross-section distribution

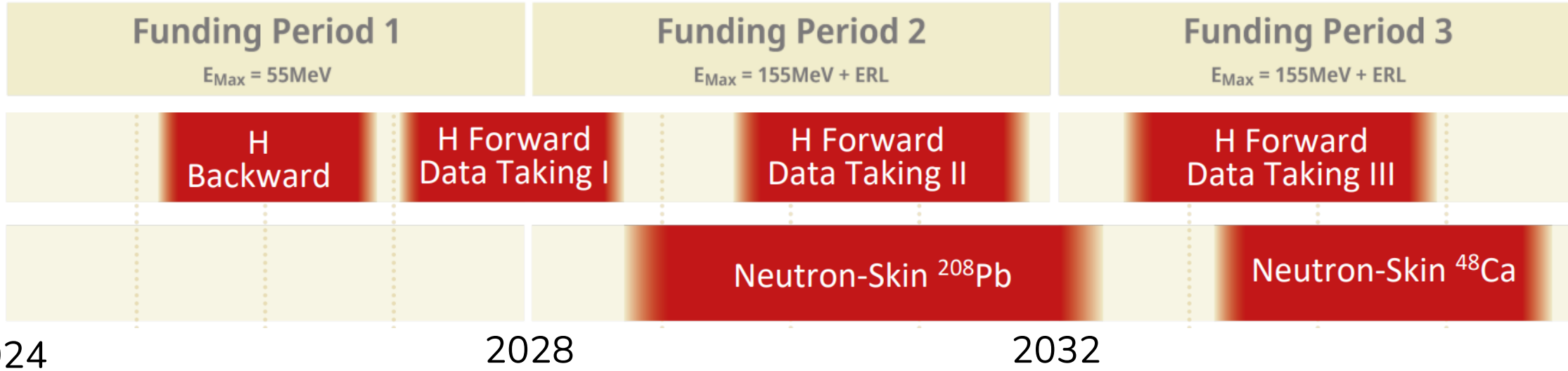


Asymmetry distribution

Optimal target position and shielding



Timing



October 2023: Cooling system installed



April 2024: Beam at the end of the LINAC



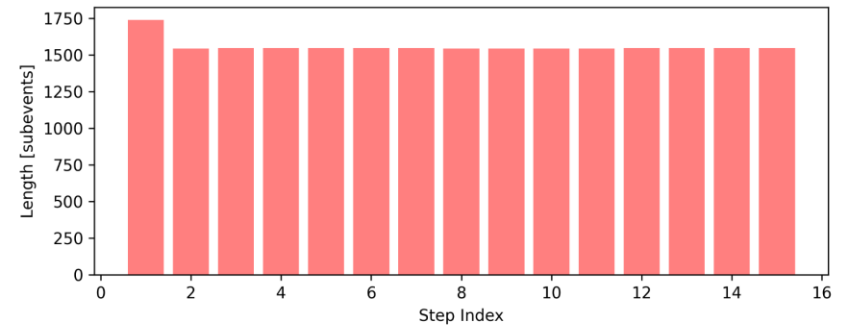
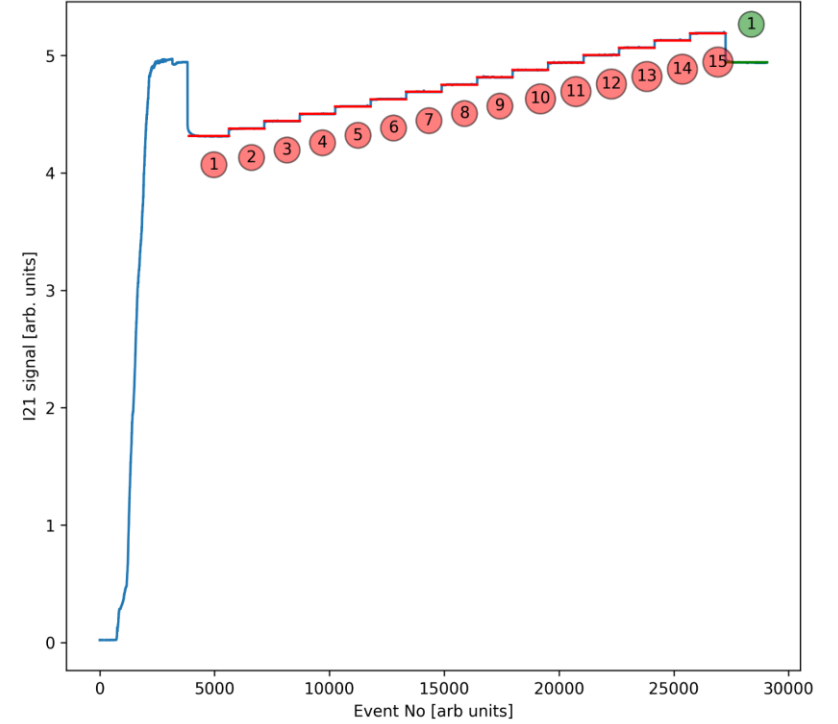
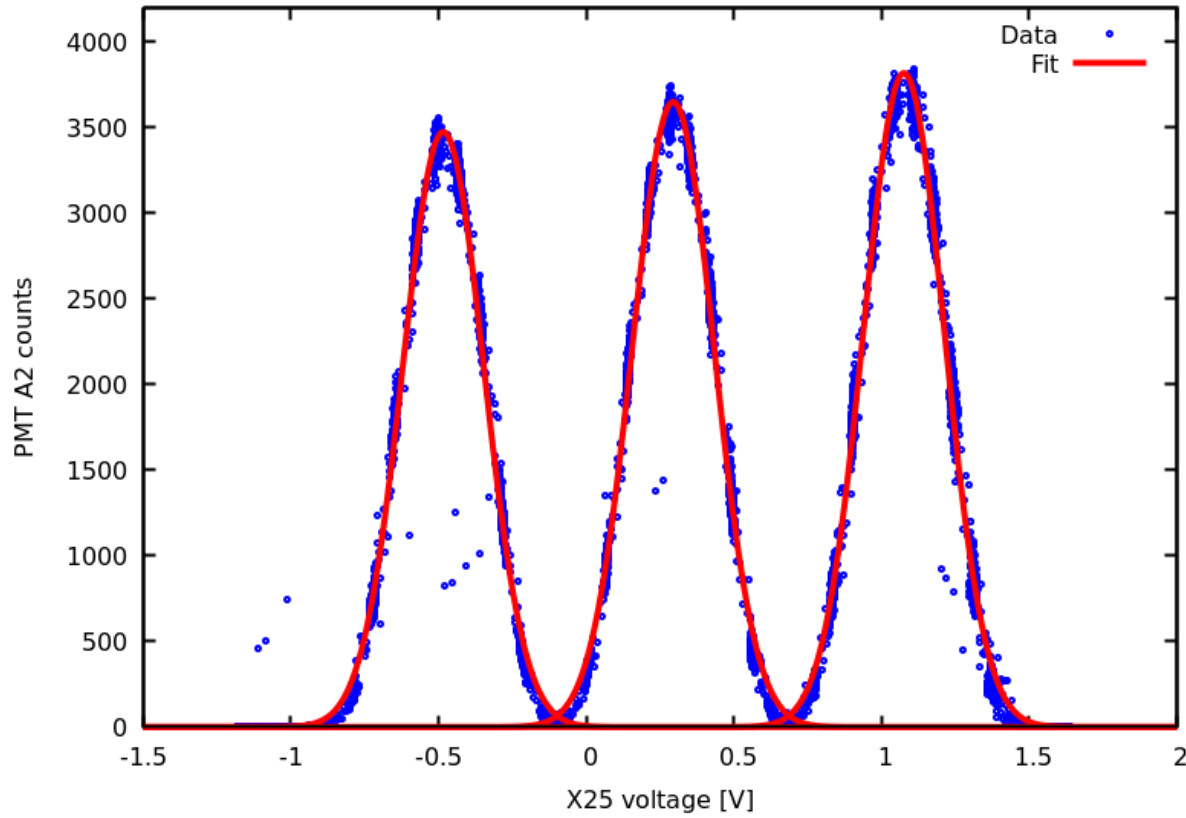
June 2024: Most of the high-frequency power amplifiers put into operation

A1 systematics

Spectrometer	A	B
Scattering angle	20.14 °	20.56°
Q^2 (GeV ² /c ²)	0.040	0.041
A_n (ppm)	8.954	9.568
$\Delta(\partial\sigma/\partial x)$	< 0.001	< 0.001
$\Delta(\partial\sigma/\partial y)$	0.012	0.009
$\Delta(\partial\sigma/\partial x')$	< 0.001	0.006
$\Delta(\partial\sigma/\partial y')$	0.012	0.003
$\Delta(\partial\sigma/\partial E)$	0.031	0.018
ΔA_I	0.008	0.008
ΔGain	0.034	0.016
ΔTails	0.145	0.034
$\Delta\text{Inversion}$	0.026	0.074
$\Delta\text{Analysis}$	0.029	0.611
ΔP	0.109	0.117
Total systematic error	0.192	0.628
Statistical error	2.416	4.331

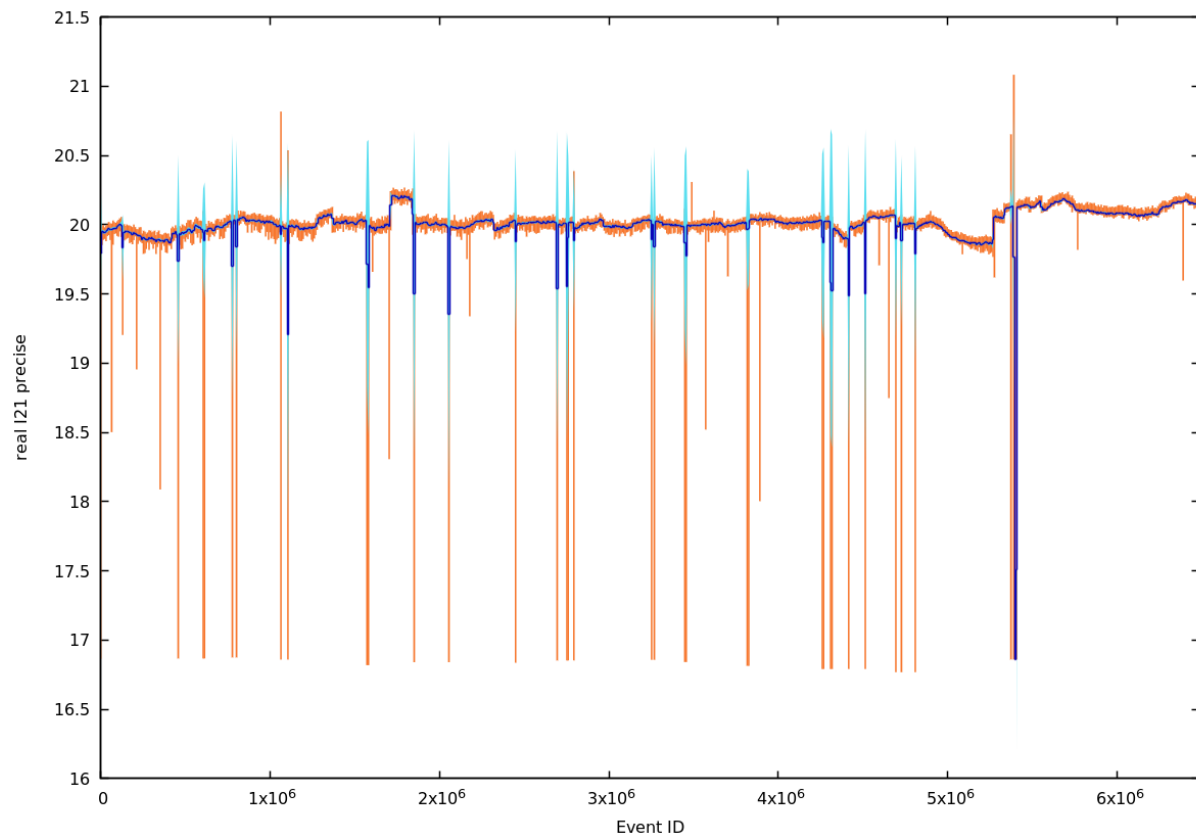
TABLE I. Measured beam-normal single-spin asymmetries for each spectrometer. The difference in scattering angle at similar Q^2 arises from the broader angular acceptance of spectrometer A. Uncertainties are in parts per million (ppm), with statistical and systematic contributions listed separately. The first five entries correspond to asymmetry correction errors. Further contributions: ΔA_I estimates the residual beam-current asymmetry, ΔGain assesses PMT gain variations, ΔTails estimates for nonlinearities from large corrections, $\Delta\text{Inversion}$ accounts for the different number of events in both states of the half-wave plate, $\Delta\text{Analysis}$ quantifies the spread between the two independent analysis chains and ΔP gives the polarization uncertainty.

A1 calibrations

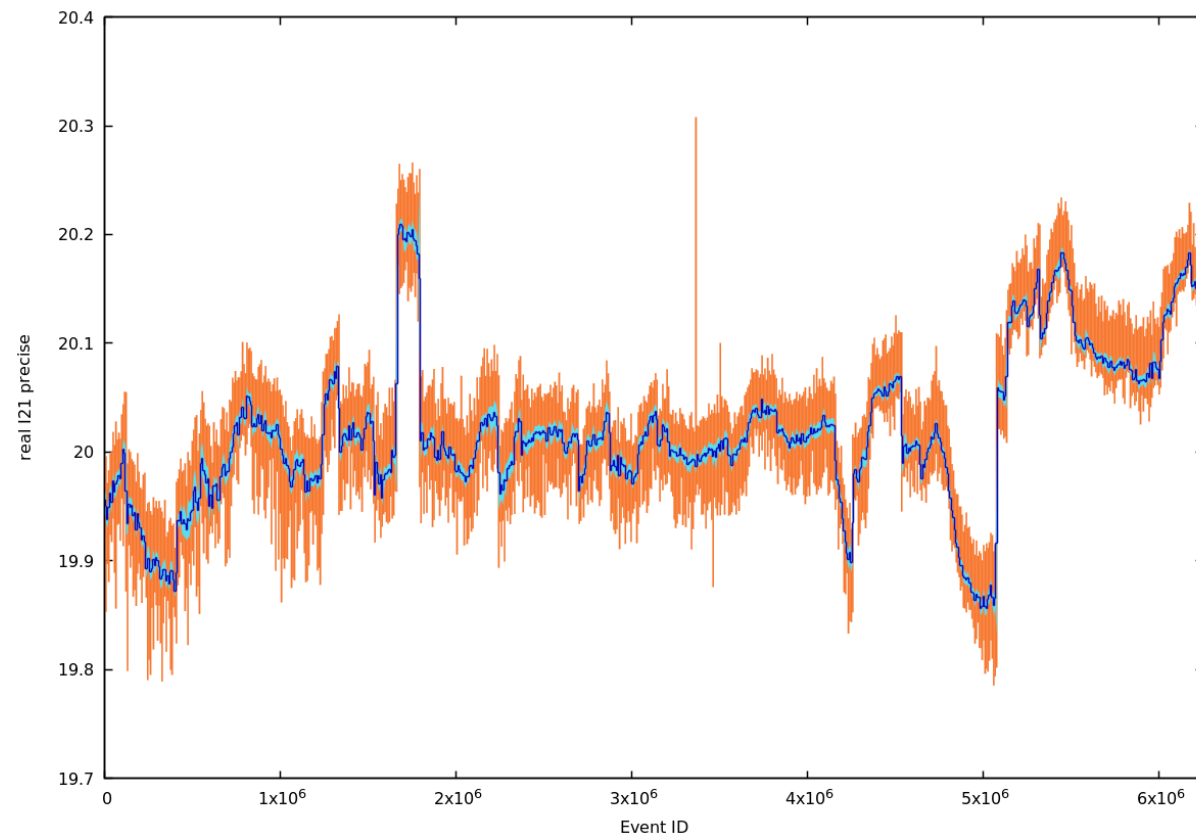


Manual cuts (clean-up)

June before manual clean-up



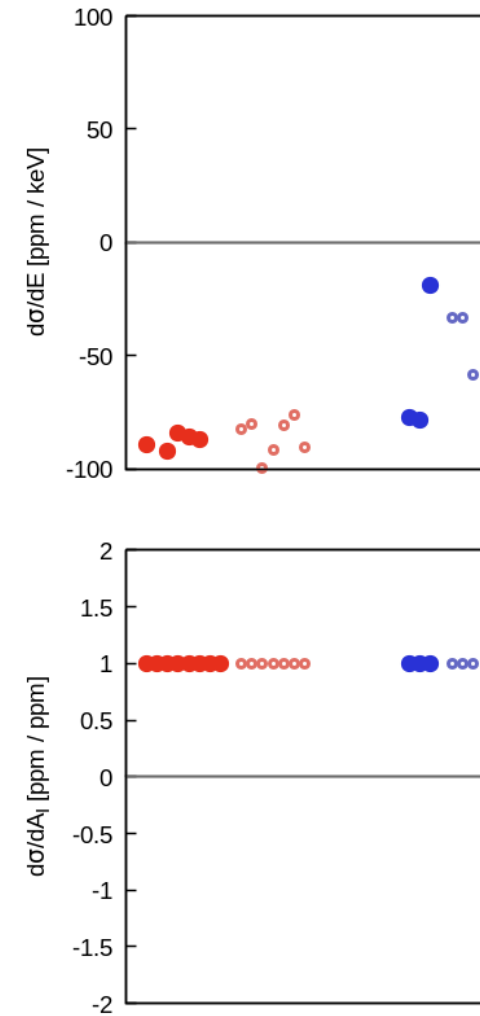
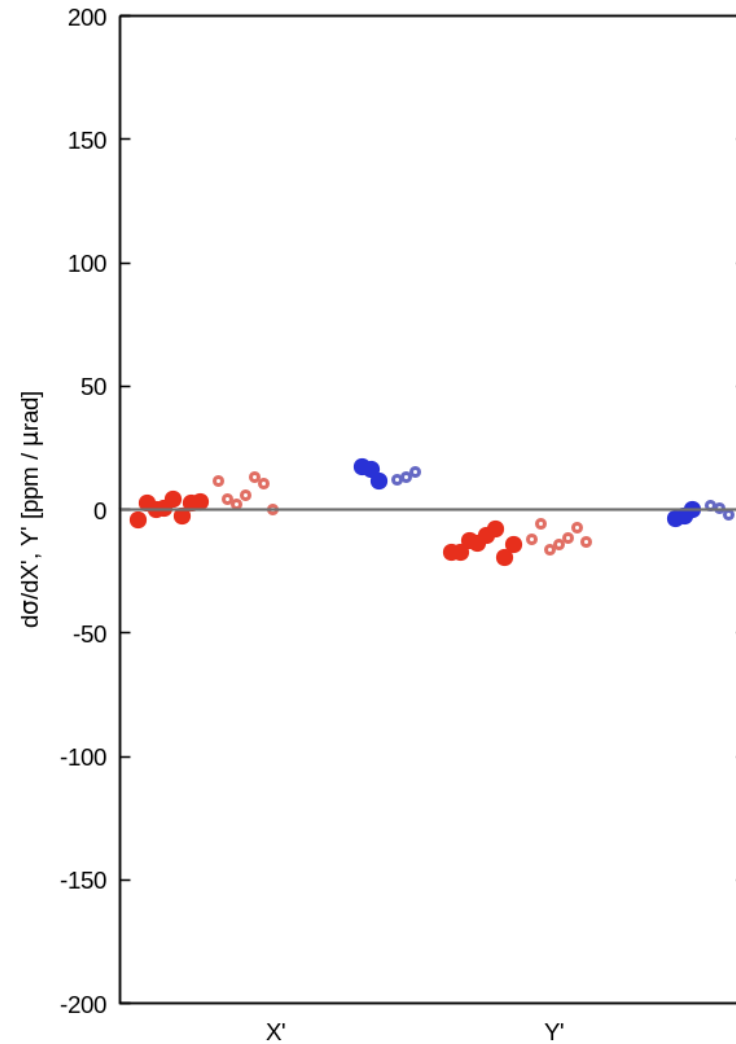
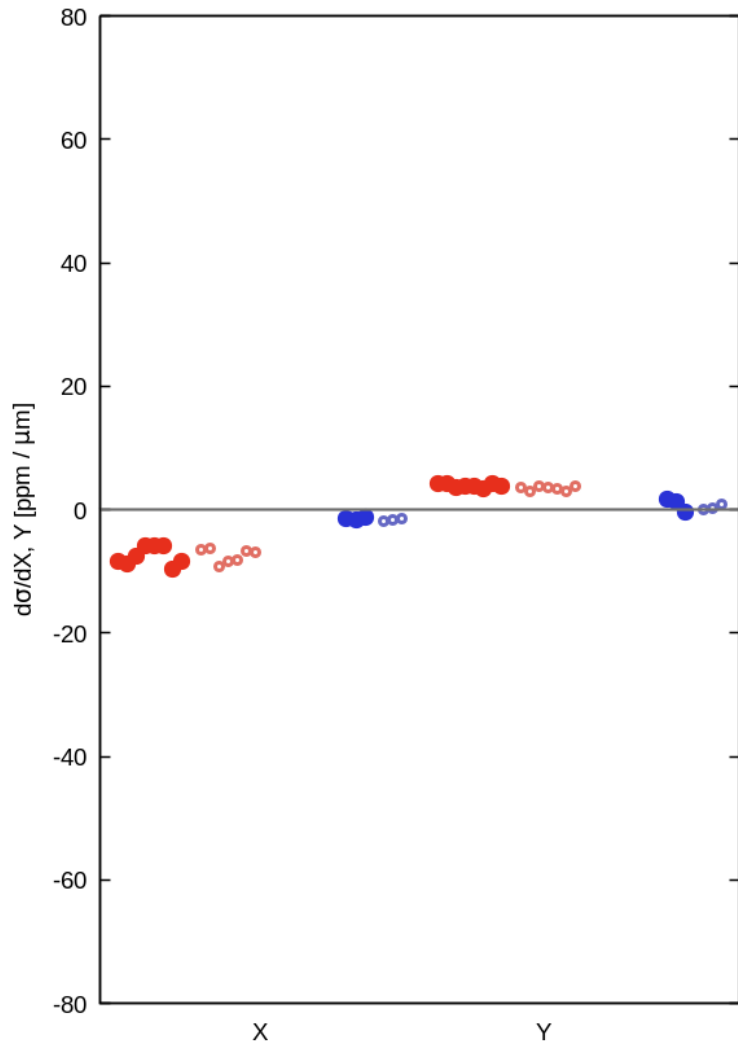
June after manual clean-up



234180 (3.6%) events cut out

Corrections

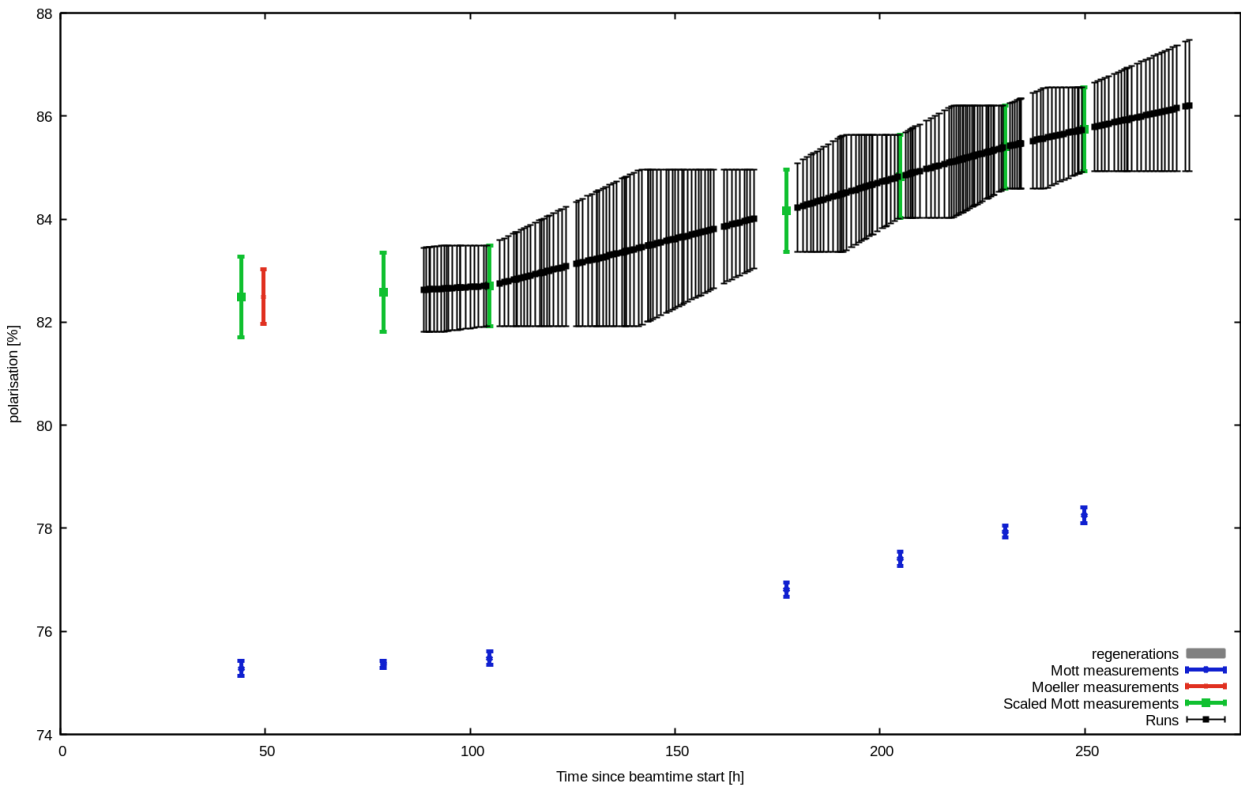
$$A_{\perp} = \frac{1}{P_{\perp}} \left(A_{raw} - c_I A_I - \frac{\partial \sigma}{\partial X} \Delta X - \frac{\partial \sigma}{\partial Y} \Delta Y - \frac{\partial \sigma}{\partial X'} \Delta X' - \frac{\partial \sigma}{\partial Y'} \Delta Y' - \frac{\partial \sigma}{\partial E} \Delta E \right)$$



June

Beam Polarisation

June



November

